Department of Food Science and Human Nutrition
Agricultural
University of Athens

Master's Thesis
MSc Direction in Food Science and Technology and Human Nutrition:
Food Bioprocesses and Biorefineries

Electrodialysis (ED) study for the recovery of short chain carboxylic acids - Mathematical modeling of the electrochemical process.

Author:
Sofia Pappa

Supervisor:
Prof. Apostolos Koutinas
Co-supervisor:
Prof. Ioannis Kookos

Athens, 2017

Master's Thesis

MSc Direction in Food Science and Technology and Human Nutrition:
Food Bioprocesses and Biorefineries

Electrodialysis (ED) study for the recovery of short chain carboxylic acids - Mathematical modeling of the electrochemical process.

Author:
Sofia Pappa

Jury committee
Prof. Apostolos Koutinas
Prof. Ioannis Kookos
Prof. Seraphim Papanikolaou

Athens, 2017

Abstract

In this thesis, the recovery of four short-chain carboxylic acids (succinic, formic, lactic, acetic acid) was examined *via* electrodialysis. Ions were able to cross this membrane easily under the applied potential gradient of 0.57 A. The flux of the acids was depended on the initial concentrations. At 10h of the process about 93.2% recovery of succinic acid was achieved when the initial concentrations was 0.25 M. At 6-7 h of process 94.5%, 95.6%, 85.6% for acetic acid, formic acid and lactic acid was recovered, respectively.

In addition, the energy consumption and current efficiency values for the recovery of the four carboxylic acids were in between 4.8 - 6.3 kWh/kg and 95.3%, respectively for succinic acid 0.25 M, 8.26 - 10.84 kWh/kg and 74.3% for acetic acid, 4.9 - 6.2 kWh/kg and 71.3% for formic acid and 4.58 - 8.75 kWh/kg and 87.8% for lactic acid. The acid fluxes were calculated and we observed that for each acid the flux values (J) have a linear relationship to the electric quantity through the membrane cell and the J values increased at higher concentrations.

From the experimental data, a prediction model of the concentration values based on the current and a dynamic model based on the electrodiffusion theory was formed. Four equations one for each carboxylic acid are presented for the prediction of acid concentrations. Those equations describe really well the recovery of the four carboxylic acids as we observed when we compared them with the experimental data. Thus, those equations can be very usefull in future experiments as a guide.

For succinic acid :

$$R = 10.2 + \frac{4.3}{C^{0.29}} \ . \tag{1}$$

For acetic acid:

$$R = 10.1 + \frac{7.2}{C^{0.47}} \ . \tag{2}$$

For formic acid:

$$R = 10.1 + \frac{0.15}{C^{1.4}} \ . \tag{3}$$

For lactic acid:

$$R = 10.3 + \frac{2.06}{C^{0.7}} \ . \tag{4}$$

All the models presented in this thesis were able to fit the experimental data quite well and can be employed for use and prediction of batch electrodialysis for carboxylic acid's recovery. Predictions were made for the concentrations in the anolyte and in the catholyte, for volumes, voltage, power and energy consumption.

The realization that life is absurd cannot be an end, but only a beginning.
Albert Camus

To my best friends who are my family...

To my father, my mother and my brother who have always been and will always be my best friends...

Acknowledgement

Communication in a foreign language can be tricky. As it is well known, our language is the reflection of ourselves and thus I would prefer the acknowledgments to be in my mother tongue.

Αρχικά θα ήθελα να ευχαριστήσω ιδιαίτερα τους υπεύθυνους καθηγητές μου Γ.Κούκο και Α.Κουτίνα για την υπομονή, τις συμβουλές τους και την καθοδήγησή τους, καθώς και την υποψήφια διδάκτορα Χ.Πατεράκη για την συνεχή βοήθεια που μου παρείχε.

Ένα μεγάλο ευχαριστώ σε όλους στο εργαστήριο της Μηχανικής Τροφίμων που με βοήθησαν ο καθένας με τον τρόπο του. Τον καθηγητή κ. Σ. Παπανικολάου που ήταν καθόλη την διάρκεια του μεταπτυχιακού προγράμματος δίπλα μας, και από καρδιάς τα ¨κορίτσια μου¨, το Μαράκι, την Έφη, την Κατιάνα, την Έλενα, την Ελένη, την Έλενη και την Όλγα που έκαναν την διαδικασία του μεταπτυχιακού πολύ ευχάριστη και απέδειξαν για μια ακόμη φορά πως η αλληλεγγύη και η συντροφικότητα μόνο καλό μπορούν να φέρουν.

Τέλος επειδή με την ολοκλήρωση της παρούσας εργασίας κλείνει ένα μεγάλο κεφάλαιο της ζωής μου, αυτό των φοιτητικών μου χρόνων δεν θα μπορούσα να μην ευχαριστήσω τους ανθρώπους που με συντρόφευσαν σε αυτό το ταξιδι και συνέβαλαν στο να γίνω ο άνθρωπος που είμαι σήμερα.

Τους αγαπημένους μου φίλους, ιδιαίτερα τη Χριστίνα, τη Φραν, την Εύα και την Δανάη που με στήριζαν άνευ όρων κάθε φορά που το χρειαζόμουν και μου θύμιζαν πως σημασία έχει το ταξίδι και όχι η Ιθάκη (παρότι την έχουμε και αυτή σε μεγάλη εκτίμηση!).

Την οικογένεια μου που δεν με άφησε ποτέ να αισθανθώ μόνη.

Και τέλος θα ήθελα να ευχαριστήσω όλους αυτούς που συνέβαλαν στο να μάθω να αγαπώ το διάβασμα!

Σ.

Contents

List of Figures

List of Tables

Chapter 1

Introduction

Electrodialysis (ED) and its applications are discussed in this Chapter for the recovery of short-chain carboxylic acids (SCCAs). Our aim is to introduce the fundamental concepts and laws of ED. One of the most interesting things about electrochemistry, is the fact that it combines kinetics, transport phenomena and thermodynamics. This field is extremely challenging.

1.1 Ion exchange membrane processes

When referring to membrane separation technology we mean the partial separation of a mixture of two or more components by the use of a semi-permeable barrier. Driving forces can be hydrostatic pressure, concentration or electrical potential. Ion exchange membranes are used in a number of separation processes, the most important of which is electrodialysis (Fig. 1.1). Over the last decades, the membrane technology and the number of people dealing with membranes is growing rapidly [9].

Anion-(AEM), cation-exchange(CAE) or bipolar (BPM) membranes are typically arranged in an alternating pattern between two electrodes (an anode and a cathode) within

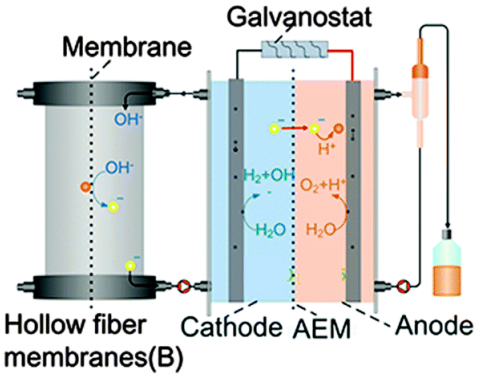

Figure 1.1: Mechanism of anion transfer and collection in a membrane electrodialysis cell (Xu et al.,2015) [2].

the electrodialysis stack. A galvanic potential is supplied as a voltage generated at the electrodes. Ion-exchange membranes are made of a polymeric material attached to charged ion groups.

The selectivity of the membranes is due to Donnan equilibrium (Section 1.6) and Donnan exclusion [10]. The latter, is the reduction of concentration of the ions in the membrane due to other ions with the same charge.

The most desired properties required for successful ion-exchange membranes are: high permeselectivity, low electrical resistance, good mechanical stability and high chemical and thermal stability and low production costs [11].

Different types of separation exist and they require a different amount of energy [9]. In a membrane separation process, various driving forces can activate the transport rate of a component, such as gradients in concentration, pressure, temperature or electrical potential.

In most of the separation processes more than one driving force is involved, for example concentration and electrical potential in electrodialysis. However, these parameters can be included in one thermodynamic function, the electrochemical potential n, which includes the chemical potential. Thus, the flux J can be described:

$$J_i = -L\frac{dn_i}{dx}, \tag{1.1}$$

where $\frac{dn_i}{dx}$ is the gradient in electrochemical potential of the component I, and L is a phenomenological coefficient [12].

In multi component systems, driving forces and fluxes are interdependent. Thus eq. 1.1 becomes more complex:

$$J_i = -L_{ij}\frac{dn_i}{dx}, \tag{1.2}$$

where L_{ij} is a proportionality coefficients.

1.2 Introduction to electrodialysis (ED)

Electrodialysis (ED) is one of the main growing applications of membrane technology. ED is a form of dialysis in which the rate is increased by the presence of an electric potential across the membrane and ions are transported through the ion selective membrane.

ED comprises conventional electrodialysis (CED), electrometathesis (EMT), electro-ion substitution (EIS), eletro-ion injection-extraction (EIIE), electro-electrodialysis (EED), electrohydrolysis with bipolar membranes (EDBM), electrodeionisation (EDI), and two-phase electrodialysis (TPED) [13].

Electrodialysis takes place in a configuration called the electrodialysis cell. The cell consists of two compartments and an ion exchange membrane is placed between two electrodes. The membrane in monopolar ED is cation-(CM) or anion-selective (AM), which means that either positive or negative ions will flow through due to the Donnan repulsion as it is shown in Fig. 1.2. The other type of ion-exchange membrane is the bipolar

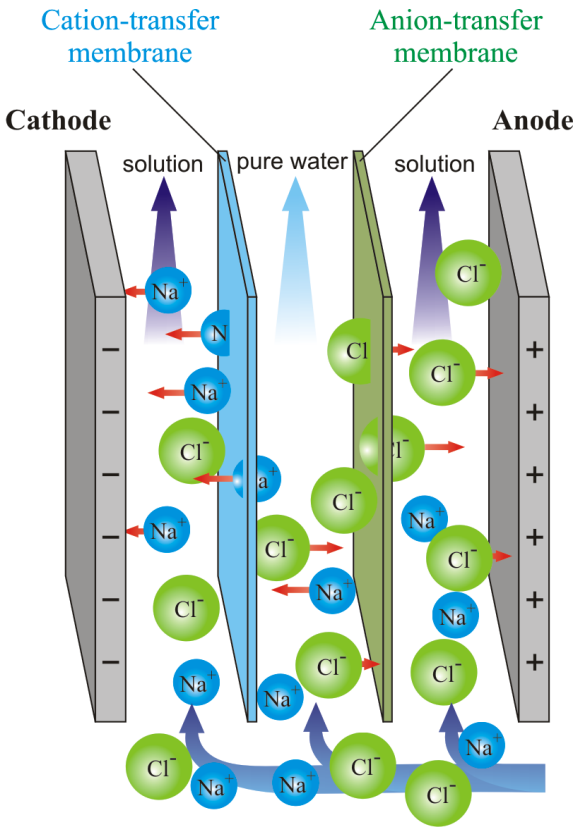

Figure 1.2: Electodialysis (Generalic, 2017) [3]

membrane (BM), which is a composition of a cation-selective layer and an anion-selective layer.

Direct electric field on the membrane between the electrodes, is the driving force at the ED process. While apllying electric field and electric current into the system an electrochemical reaction takes place at the electron solution interface. Thus oxygen formation and reduction of protons to hydrogen takes place in the anode and in the cathode, respectively as we can see in Fig. 1.3. The migration movement of all ions disolved in this process is due to the applied electric field, thus the cations move towards the anode, while anios towards cathode. This movement is indicated as an electric current flow throught the ED stack and the ions meet ion-selective membranes on this way. During the ED process the concentration, and consequently electric conductivity, of the solution in the dilute stream decreases resulting in the increase of the electric resistance of the ED unit. In the galvanostatic operation mode this could lead to uncontrolled increase of voltage applied on the ED unit. Industrial size electrodialysis stack consits of 100-200 cell pairs that are arranged between the electrodes. Additionally various spacer and stack constructions such as sheet flow and tortuous path flow stack design are used in many applications. In the latter case, the membranes and the spacers are placed horizontally in a stack, thus in the sheet flow spacer the compartments are verically arranged and the process path is relatively short.

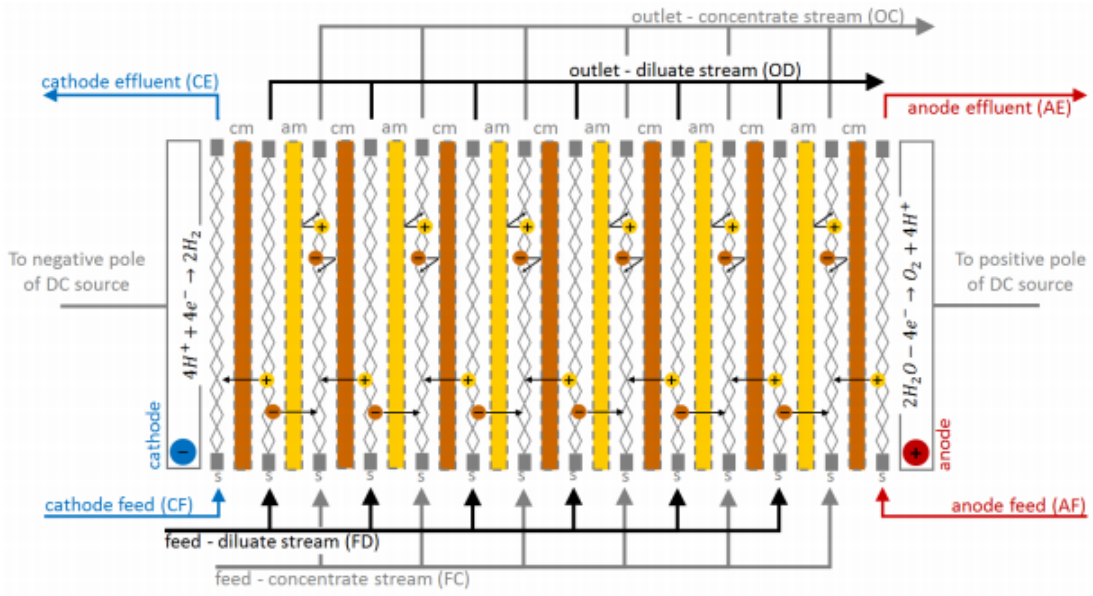

Figure 1.3: Schematic sketch of the ED process (Nemecek M. et al., 2017) [4]

The spacers, apart from separating the membranes, they also contain the manifold for the distribution of the two different flow streams in the stack and to provide a proper mixing of the solutions [11].

ED appears for the first time in educational literature in 1931 [12] but many scientists, before that, had applied the method in research as well as in the industry. Experiments with ion exchange membranes were described as early as 1890 by Ostwald [14] and the work by Donnan [15] a few years later led to development of the concept of membrane potential and the phenomenon of Donnan exclusion. Kendall and Gebauer-Fuelnegg, presented three reasons why electrodialysis is a "neglected method". Apparently, since 1931 huge improvements have been made and we can no longer consider electrodialysis a neglected method and the increasing interest in electrochemical education is reflected by numerous publications in the last years.

CED has been used for several decades for several industrial applications. The most common applications are the desalination of brackish water [16] and the electrolytic production of chlorine and caustic soda [17]. From waste water treatment [18] to fruit juice de-acidification, to the demineralisation of whey for baby food industry and to the production of table salt [17] CED is used widely. It can also be used in drug and chemical industries with several applications, such as the recovery of mixed acid and base from wastewater [19] and the extraction of medium-chain carboxylic acids (MCCAs) from bioreactor broth [2] and the recovery of short-chain carboxylic acids (SCCAs).

Apart from Electodialysis, which still remains the most important industrial membrane separation technology using ion-exchange membranes with electrical potential as a driving force, there are several other processes with a good industrial significance, such as

chlorine- alkali electrolysis, diffusion dialysis, Donnan dialysis, electrodialytic regeneration of a cation- or anion-exchange resins and hybrid processes.

As we mentioned before, the process of ED takes place in a configuration called, electrodialysis cell. An electrodialysis cell can be described by the laws of electrochemistry.

Electrochemistry is a field of physical chemistry that deals with the study of reactions that either consume or generate electricity. These reactions are called electrochemical reactions. Electrochemical processes are carried out in numerous technological and industrial applications. Manufacture of inorganic chemicals, synthesis of organic compounds, extraction of metals, recycling of chemicals and process streams, chemical purification and separation, water and effluent treatment, total destruction of toxic materials, soil remediation, atmosphere control, metal finishing, manufacture of electronic components, metal fabrication, batteries' fuel cells and sensors are some of the industrial applications of electrochemistry. Electrochemical systems deal with processes and factors that affect the transport of charged molecules across the interface between chemical phases, for example, between an electronic conductor (an electrode) and an ionic conductor (an electrolyte) [20].

The generation or the consumption of electrical power is always associated with the production of current flow, i.e. the electron flow. Thus, the typical chemical reaction at an electrolyte solution in which we observe changes in the electrical charge can be described by the following:

$$A^{zA} + B^{zB} <=> A^{zA-n} + B^{zB-n}, \tag{1.3}$$

where zA and zB are the charge numbers of A, B and n>0 the number of electrons exchanged during the chemical reaction.

In ED at the negative electrode (cathode) hydrogen (H_2) and hydroxyl ions (OH^-) are

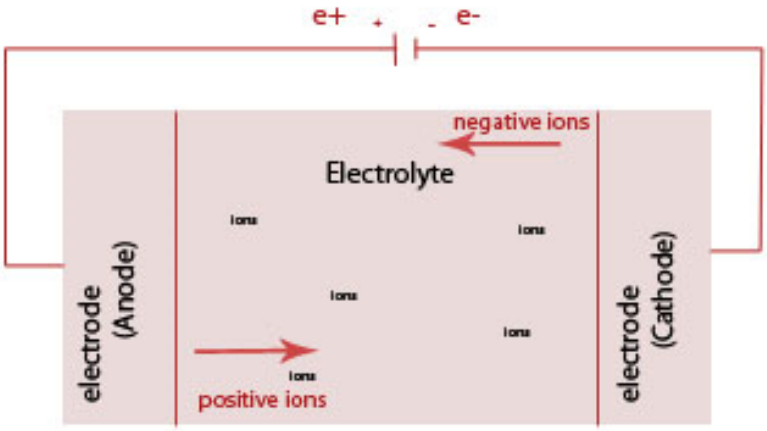

Figure 1.4: Electrochemical system

being produced, whereas oxygen (O_2) and hydrogen ions (H^+) are produced in the positive electrode (anode) [9]:

$$2e^- + 2H_2O => H_2 + 2OH^-, \tag{1.4}$$

$$H_2O => \frac{1}{2}O_2 + 2H^+ + 2e^-, \tag{1.5}$$

Electrochemical reactions always take place at the interface between the electrode and electrolyte. The application of the Voltage (V) is the key to driving an electrode reaction:

$$V = Joule/Coulomb \tag{1.6}$$

where we can see that one volt is simply the energy (J) required to move the charge (c). Therefore, the application of a voltage to an electrode supplies electrical energy. Since electrons possess charge, an applied voltage can alter the "energy" of the electrons within a metal electrode.

1.3 Mass transfer in ED

Mass transport in electrodialysis can be described, under the assumption of ideal solutions, nor pressure gradients nor kinetic coupling or fluxes. And expressing the phenomenological coefficient by Maxwell-Stefan diffusion coefficient, the flux Ji of the i^{th} ion is:

$$J_i = -D_i(\frac{dc_i}{dx} - c_i \sum_{i=1}^{n} \frac{T_i}{c_i}\frac{dc_i}{dx}) + T_i\frac{I}{z_iF} \tag{1.7}$$

where D_i is the diffusion coefficient, c_i the concentration, T_i the transport number, z_i the valence of i^{th} ion, x the axial coordinate, I the current and F the Faraday constant.

The transport number T_i determines the fraction of the current carried out by i-th ion.

$$T_i = \frac{z_iJ_i}{\sum_{i=1}^{n} z_iJ_i} \tag{1.8}$$

In strictly permeselective AEM the current is transported by anions, and in CEM the current is transported by cations only.

The current I, is related to the flux and can be described by the following equation:

$$I = F\frac{z_iJ_i}{\sum_{i=1}^{n}} = z_i, J_i \tag{1.9}$$

Three types of transport phenomena exist in an electrochemical system, diffusion, convection and migration. Thus, in all electrochemical cells more than one transport process is taking place and each type of transport influences the others [5].

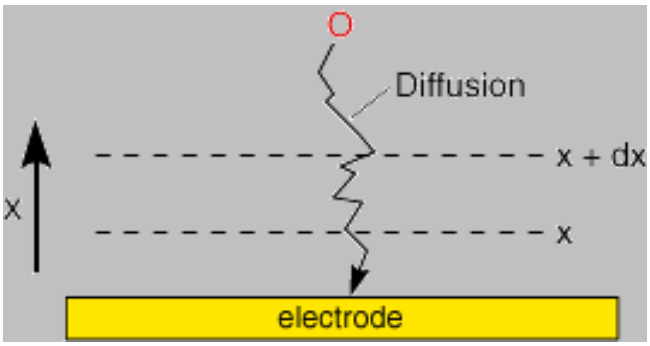

Figure 1.5: Diffusion, (Fisher, 2017) [5]

- **Diffusion**, occurs in all solutions and arises from local uneven concentrations of reagents. Entropic forces act to smooth out these uneven distributions of concentration and are therefore the main driving force for this process Fig. 1.5.

  Diffusion is particularly significant at ED since the conversion reaction only occurs at the electrode surface. Consequently there will be a lower reactant concentration at the electrode than in bulk solution. Similarly a higher concentration of product will exist near the electrode than further out into solution.

  The rate of transfer by diffusion can be predicted mathematically and Fick proposed two laws to quantify the processes. The first law,

$$J_o = D_o(\frac{\partial C_o}{\partial x}) \tag{1.10}$$

  relates the diffusional flux Jo (i.e. the rate of transfer of material by diffusion) to the concentration gradient and the diffusion coefficient Do. The negative sign simply signifies that material moves down to a concentration gradient (i.e. from high to low concentration). The concentration of the material varies as a function of time which can be predicted from the first law.

  That results to Fick's second law:

$$\frac{\partial C_o}{\partial t} = D_o(\frac{\partial^2 C_o}{\partial x^2}) \tag{1.11}$$

  In this case we consider diffusion normal to an electrode surface (x direction). The rate of change of the concentration ($[C_o]$) as a function of time (t) can be seen to be related to the change in the concentration gradient. So the steeper the change in concentration the greater the rate of diffusion.

  Fick's second law establishes an important relationship since the prediction of the variation of concentration of different species as a function of time within the electrochemical cell is feasible. In order to solve these equations analytical or computational models are usually employed.

- **Convection** results from the action of a force on the solution. This can be a pump, a flow of gas or even gravity. There are two forms of convection the first is termed natural convection and is present in any solution. This natural convection is generated by small thermal or density differences and acts to mix the solution in a random and therefore unpredictable manner. In the case of electrochemical measurements these effects tend to pose problems if the measurement time for the experiment exceeds 20 seconds.

  The mass transport equation for (1 dimensional) convection and laminar flow conditions is predicted by:

$$\frac{\partial C_o}{\partial t} = -v_x(\frac{\partial C_o}{\partial x}) \tag{1.12}$$

  where v_x is the velocity of the solution which can be calculated in many situations be solving the appropriate form of the Navier-Stokes equations. An analogous form exists for the three dimensional convective transport. When an electrochemical cell possesses forced convection we must be able to solve the electrode kinetic, diffusion and convection steps, to be able to predict the current flowing. This can be a difficult problem to solve even for modern computers and yet we still have one final form of mass transport to address!

- **Migration**. The final form of mass transport we need to consider is migration. This is essentially an electrostatic effect which arises due the application of a voltage on the electrodes. This effectively creates a charged interface (the electrodes). Any charged species near that interface will either be attracted or repelled from it by electrostatic forces. The migratory flux induced can be described mathematically (in 1 dimension) using

$$\frac{\partial C_o}{\partial t} = -uC_o(\frac{\partial \emptyset}{\partial x}) \tag{1.13}$$

  However due to ion salvation effects and diffuse layer interactions in solution, migration is notoriously difficult to calculate accurately for real solutions. Consequently most voltammetric measurements are performed in solutions which contain a background electrolyte - this material is a salt (eg KCl) that does not undergo electrolysis itself but helps to shield the reactants from migratory effects. By adding a large quantity of the electrolyte (relative to the reactants) it is possible to ensure that the ED reaction is not significantly affected by migration. The purpose of introducing a background electrolyte into a solution is not however solely to remove migration effects as it also acts as a conductor to help the passage of current through the solution[5].

1.4 Concentration polarisation and limiting current density

In ED high current results in fast process with the lowest possible effective membrane area. In practice, however, operating currents are restricted by the occurrence of the concentration polarisation phenomena. The concentration polarisation is the result of the difference between the transport numbers of ions in the membrane and in the solutions. The transport number of a counter - ion in an ion - exchange membrane is generally close to one and that of the co - ion is close to zero. Concentration polarisation in electrodialysis leads to an accumulation of ions on the membrane surface facing the concentrate compartment. In the dilute cell the concentration polarisation leads to a depletion of ions at the membrane surface and determines the so-called limiting current density which is reached when the ion concentration at the membrane surface approaches to zero [11].

An effective method to study the transport of ions through an anion exchange membrane is by determining so-called current - voltage curves [21]. These curves show the relationship between the current through our membrane and the simultaneous voltage drop across membrane.

Additionally, the limiting current density can be calculated by a mass balance taking into account all fluxes in the boundary layer and the hydrodynamic conditions in the flowchannel between the membranes.

In Fig. 1.6 we can see a typical example of the current - voltage curve. The are three distingt phases: the ohmic (A), the limiting current (B) and the electroconvection (C). In the ohmic phase (A) at low current densities there is a linear relationship between the current and the voltage drop according to Ohm's law. From the above information, we can make the conclusion that the penetrating flux of ions through the anion exchange membrane (AEM) increases linearly with the electric field. At the limiting current phase (B), the concentration of ions reaches zero at the membrane interface (polarisation) and the resistance tends to infinity. This phenomenon occurs due to the fact that the flow rate of the ions through the membrane is faster than the flow rate of the molecular diffusion. Under those circumstances, the electrodialysis current density remains steady and the diagram shows a pesudo-plateau. Subsequently, as the electric voltage increases at the electroconvection region (C), the interface between the electrolyte and the membrane gets hydrolysed and a large amount of H^+ and H^- ions in the solution is released.

The electrodialysis takes place within the ohmic region as the current efficiency is reduced in the limiting current region. Nevertheless, recent research shows that the electrodialysis is more effective in the electroconvection region due to the acceleration of the ions migration [22].

1.5 Voltage requirements

Voltage requirements for an ED system depend on current resistance. The current is determined by Faraday's Law and the resistance is determined by the components of the membrane stack and the solution according to Ohm's Law [23].

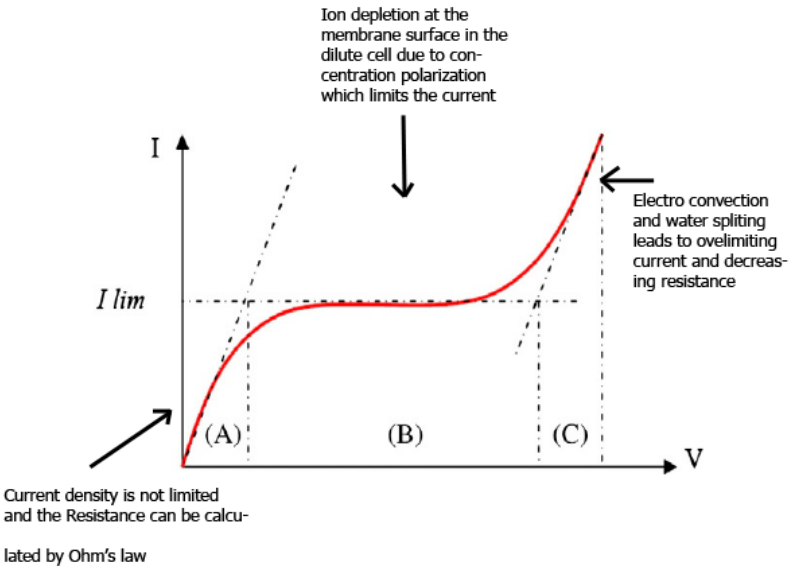

Figure 1.6: Current-voltage curves (Ridha et al., 2014)[6].

1 Ohm's Law

Ohm's law states that the direct current flowing in an electric circuit is directly proportional to the voltage applied, and inversely proportional to the resistance of the element:

$$I = \frac{V}{R} \tag{1.14}$$

The overall resistance of the ED process can be affected by the resistance of the ion exchange membrane, the resistance in the anolyte and the catholyte, the temperature, the conductivity and the ionic composition of the solutions. The components that contribute to membrane resistance are expressed by the following equation:

$$R_{ep} = R_{em} + R_{am} + Rc + R_d \tag{1.15}$$

where, $R_{ep}(\Omega/cm^2)$ is the resistance per unit area of one cell pair,$R_{em}(\Omega/cm^2)$ the resistance per unit area of cation membrane, $R_{am}(\Omega/cm^2)$ the resistance per unit area of anion membrane, $R_c(\Omega/cm^2)$ the resistance per unit area of concentration stream and $R_d(\Omega/cm^2)$ the resistance per unit area of dillute stream.

2 Faraday's Law

The ED process is related to Faraday's Law. The needed current for transferring a specific quantity of salt is given by the equation :

$$I = \frac{F\Delta C}{Nn} \tag{1.16}$$

where F = 96485 C·mol^{-1}, is the Faraday constant that indicates that the 96.485 Ampere transfers theoritically one gram-equivalent of salt. Faraday's Law is used to relate the transfer of salts through the membranes and the amount of current flowing through the membranes. This shows that the amount of current required is directly proportional to the flow rate through the diluting compartments and the amount of ionic equivalents to be removed, and inversely proportional to the current efficiency.

1.6 Energy consumption & current efficiency

One of the most important factors to measure the efficiency of an electrodialysis process is the current efficiency and the energy consumption.

The current efficiency is an expression of the amount of electrical energy added to the system that is being utilized for the targeted separation. The current efficiency is a combination of the selectivity of the membrane (Donnan exclusion), the pH of the feed solution, back diffusion of already transferred ions and current leakage in the system.

In ED processes there are two energy requirements. The first one is the electrical energy needed to transfer the ionic components from one solution to another and the second requirement is the energy to pump the solutions through the electrodialysis unit [17]. In this thesis we calculated only the energy neede to transfer the ionic components we consider the other negligible.

The energy consumption is calculated according to:

$$W = \int_0^t \frac{VIdt}{w} \tag{1.17}$$

where V is the applied voltage, I the current, t is the time allowed for the electrochemical process, and w is the weight of the acids formed in the anolyte.

Current efficiency is calculated according to:

$$CE = \frac{zFQ_f(C_inlet - C_outlet)}{NI} \tag{1.18}$$

where z is the charge of the ions, F the Faraday constant (26,8 Ah), Q_f dilute flow rate (L/s), C_{inlet} and C_{outlet} the dilute ED cell concentrations, N the number of cell pairs and I the current (A).

We have to consider those two variables in order to have a technically feasible, but economically viable process [24].

1.7 The Donnan equilibrium

In electrodialysis processes, an electrical current is applied to drive ions through ionselective membranes. To obtain high current efficiencies, the ratio of counter- over co-ions permeating the membrane should be as high as possible. This ratio is related to the diffusion of the ions and to the membrane density. The distribution of ions between electrolyte and membrane is governed by the electrochemical equilibrium equation.

When an electrodialysis membrane is immersed in an electrolyte, ions and water move through the two phases until equilibrium is reached. Donnan equilibrium describes the equilibrium that exists between two solutions that are separated by a membrane. The membrane is constructed in a way that allows the transport of certain ions.

After the equilibrium is reached we can define it as:

$$RTln(f_i x_i) + z_i \mathcal{F}\phi + \bar{V}_i p = RTln(\tilde{f}_i \tilde{x}_i) + Z_i \mathcal{F}\tilde{\phi} + \bar{V}_i \tilde{p} \tag{1.19}$$

which can be writen as:

$$ln(\frac{f_i x_i}{\tilde{f}_i \tilde{x}_i}) = \frac{z_i \mathcal{F}}{RT}(\tilde{\phi} - \phi) + \frac{\bar{V}_i}{RT}(\tilde{p} - p) \tag{1.20}$$

This relates the differences between the activities of $f_i x_i$ and $\tilde{f}_i$, the electrical potential $(\tilde{\phi} - \phi)$ and the pressure $(\tilde{p} - p)$ between the two phases. This is a general thermodynamic description of the Donna equilibrium. In Eq. 1.20 the tildes denote the properties in the membrane phase, those without tildes are values in the external solution. For a single elevtrolyte solution, we can write Eq. 1.20 for cations(c) and anions(a). By eliminating the potential difference this yields:

$$\frac{{x_c}^{\nu_c} {x_\alpha}^{\nu_\alpha}}{\tilde{x}_c^{\nu_c} \tilde{x}_\alpha^{\nu_\alpha}} = (\frac{\tilde{f}_{c\alpha}}{f_{c\alpha}})^{\nu} \tag{1.21}$$

and for $\nu_c = |z_\alpha|$ and $\nu_\alpha = z_c$, with :

$$f_{c\alpha} = ({f_c}^{\nu_c} {f_\alpha}^{\nu_\alpha})^{\frac{1}{\nu}} \tag{1.22}$$

and

$$\nu = \nu_c + \nu_\alpha \tag{1.23}$$

This implies that once the internal composition is known from experiment and the external activity coefficient is obtained from literature or is calculated from a model, the internal electrolyte activity coefficient can be calculated.

Knowledge of the single internal electrolyte activity coefficient, $\tilde{f}_{c\alpha}$, is not sufficient for solving equation Eq. 1.20. There we need the activity coefficients of the ions separately; these can be obtained from multicomponent solution models as those of Pitzer and Bromley. An estimate of the Donnan potential can now be obtained from Eq. 1.24, when it is solved for all ionic species i:

$$\tilde{\phi} = \phi + \frac{RT}{z_i \mathcal{F}} ln(\frac{f_i x_i}{\tilde{f}_i \tilde{x}_i}) \tag{1.24}$$

The existence of a Donnan potential is giving us the most obvious way of calculating internal activity coefficients [18].

1.8 Kohlrausch's Law

Experimental studies that were carried out, in particular by Kohlrausch, on aqueous solutions containing only one strong electrolyte (a single type of cation and anion) produced an equation that showed how the molar conductivity is a function of the electrolyte's concentration. This is shown in the following:

$$\Lambda = \Lambda^0 - Cst\sqrt{C} \tag{1.25}$$

Λ^0 gives the value for the molar conductivity extrapolated to $C = 0$, and is called the "molar conductivity at infinite dilution" of the electrolyte (in Sm^2mol^{-1}). This quantity represents the molar conductivity for an ideal system with no interactions. This empirical law has been linked to the ionic conduction model in liquid electrolytes involving electrophoretic and relaxation effects, which are found to be very strong in concentrated solutions. For a 1-1 strong electrolyte solution, the molar conductivity of an ion i is shown in the following equation:

$$\lambda_i = {\lambda_i}^0 - (A + B{\lambda_i}^0)\sqrt{C_i} \tag{1.26}$$

with $A = 60.3$ and $B = 0.229$ at $25°C$ in water, if C_i is in $molL^{-1}$ and ${\lambda_i}^0$ in Scm^2mol^{-1} ; ${\lambda_i}^0$ is called molar conductivity at infinite dilution of the ion i (in Sm^2mol^{-1}). A, B and ${\lambda_i}^0$ are temperature-dependent .

With given values of A, B, the molar conductivity of an ion can be considered as independent of the concentration, with an accuracy rate of about 5%, to its value at infinite dilution once the concentration is lower than a few 10^{-3} $molL^{-1}$ at $25°C$. In such conditions, the electric conductivity of the electrolytic solution is simply proportional to the electrolyte concentration [25].

1.9 Existing Models of ED

The development, design, and operation of electrochemical processes have seen enormous advances within the last few decades with profound changes in the recent past. In order to optimise the electrodialysis process many scientific groups tried to create suitable mathematical model describing the process.

Ever since the invention of the first ED apparatus by the Botho Graf von Schwerin in 1900 [26], the modeling of the mass transfer in an ED cell has been ambiguous. Three are the main reason for that: the determination of the properties of the ion exchange membranes, the unavailability on the membrane diffusion coefficients and the fact that the

mass transfer in an ED cell is not only of diffusive nature [27]. In this subsection we will describe the state of the art that describe the ED process.

In 1995 the electrodialysis of a NACl-HCl system and a system containing two amino acids which combined with Selemion cation exchange membranes was modeled using the Maxwell-Stefan equations by G. Kraaijeveld et al. [27]. Most of the model parameters were obtained from separate experiments or existing correlations. Four parameters were left, which were obtained by fitting the results of the electrodialysis experiments (current efficiency, convective flow and the countered ion-counter-ion diffusivity in the membrane). For each of the three resistances they had (two diffusion films and the membrane) they solved a system of partial differential equations. They indicated the fact that for an N component system, there are N-1 independent Maxwell-Stefan equations and 2N+1 unknown variables (N fluxes, N concentrations and the electrical potential) .

$$-\frac{c_i}{RT}\nabla\mu_i - \frac{z_i C_i F}{RT}\nabla\phi = \sum_{j=1}^{n}\frac{c_i c_j}{c_{tot} D_{ij}}(v_i - v_j) \tag{1.27}$$

To solve the systems of differential equations (two diffusion films and the membrane) and the Donnan equilibrium was applied.

$$K = \frac{c_+ c_-}{\bar{c}_+ \bar{c}_-} = \frac{\bar{\gamma}_\pm^2}{{\gamma_\pm}^2} \tag{1.28}$$

Finally to complete the model G. Kraaijeveld et al. described the phenomena at the electrodes and they calculated the model parameters by dividing them in two categories, membrane properties and diffusion coefficients. The Maxwell-Stefan model resulted into a very good description of the experiments.

One year later, Boniardi et al. developed a mathematical model to recover lactic acid from the fermentation broth [28]. In this work a general procedure for developing a simulation model for the electrodialysis process was presented.

Boniardi et al. outlined the fact that the ion flux through the membranes can be described by two terms: the applied electric field and to ion diffusion. As a consequence, ion and water transport through the membranes can be approximated by the following expressions:

$$J_m^\pm \cong \frac{t_m^\pm i A}{F} \tag{1.29}$$

$$N_w \cong \frac{t_m \tilde{V} i A}{F} \tag{1.30}$$

They ended with 16 equations and 16 unknowns and considered as known the current density to solve it. By using the Donnan potential difference they calculated the overall junction potential difference in the boundary layers for a cell by the following equation:

$$E_j = \frac{RT}{F}\sum_{k=1}^{4} \pm(t_k^- - t_k^+) ln \frac{C_k^{wc}}{C_k^{w\alpha}} \tag{1.31}$$

where the signs + and - refer to the product (k=1 and 3) and feed (k=2 and 4) compartments, respectively. Finally for the parameters Boniardi et al. dedicated some from the literature and those who were depended on the process (the ohmic resistance of the membranes, the mass transfer coefficient from the bulk solution to the membrane, and the difference between the electrode potentials for anode and cathode processes) they estimated them based on experimental data. To validate the model they compared it with the experimental values and there was a good agreement.

In 1998 Lee et al. [29] also developed a dynamic model for lactic acid recovery *via* ED. Based on the experimental results, mathematical models were developed, in which time changes in the feed and permeate volumes and the electrical resistance were considered. This approach is widely used since nowadays.

In order to create the prediction model Lee et al. considered the rate of ion transfer proportional to the current applied:

$$-\frac{d}{dt}(CV) = \eta\frac{NI}{zF} = \eta\frac{NAi}{zF} \tag{1.32}$$

for the volumes:

$$V = V_0 - \eta_1\frac{I}{F}\omega Nt \tag{1.33}$$

And by using eq. 1.32 and eq. 1.33 they calculated the concentration change with time by the following equation:

$$C = \frac{C_0V_0 - \eta_1(I/F)Nt}{V_0 - \eta_1(I/F)\omega Nt} \tag{1.34}$$

Finally by using Ohm's law, expressions for the time required to reach the switching point, the resistance and the energy consumption and by taking several mathematical steps they obtained eq. 1.35 and eq. 1.36 for the operations time and the energy consumption:

$$t_f = \frac{FV_0}{N}\left[\frac{C_0'c - ((1-\omega' cC_0'c)/(1-\omega' C_1'c))C_1'c}{\eta I}\right] \tag{1.35}$$

$$E = NI^2\left[\frac{F_\alpha V_0(1-\omega' cC_0'c)}{N\eta I} ln\left|\frac{C_0'cV_0}{C_0'cV_0 - (N\eta It_t/F)}\right| + (\alpha\omega' c + b)t_t])\right[\tag{1.36}$$

Although model predictions of lactate concentration, volume changes, switching time and energy consumption were in good agreement with the experimental data they came to the conclusion that in order to make the model more efficient, the behavior of electrical resistance and the current efficiency should be considered in modeling.

In 2004, Marcello Fidaleo and Mauro Moresi [30] proposed a mathematical model to assess whether ED recovery process is or is not economically feasible with respect to the precipitation process presently used by the lactic acid fermentation industry by taking into consideration also the behavior of electrical resistance and current efficiency. They calculated the differential mass and volume balances by the following equations:

$$\frac{d(C_{BC}V_C)}{d\tau} = -\frac{d(C_{BD}V_D)}{d\tau} = (t_e^+ - t_a^+)\frac{I}{F}N = (t_a^- - t_e^-)\frac{I}{F}N = t_s\frac{I}{F}N \tag{1.37}$$

$$\frac{dV_c}{d\tau} = -\frac{dV_D}{d\tau} = t_w V_w \frac{I}{F}N \tag{1.38}$$

where t_e^+,t_e^-,t_a^+ and t_a^- are the cation or anion transport numbers in cation- and anion-exchange membranes, t_s and t_w the effective solute and water transport numbers, C_AC and C_BD and are the instantaneous molar concentrations of solute in tanks C and D. V_C and $V_D$the corresponding volumes, V_w is the water molar volume, τ, I, N, F are the process time, the current, the number of cells and the Faraday constant respectively.

And for the overall stack voltage Φ :

$$\Phi = E_{el} + R_{ers}I + N(E_i + E_D + [R_b + R_f + (r_a + r_c)/\alpha_{me}]I) \tag{1.39}$$

where E_{el} is the thermodynamic potential and overpotential of electrodes, E_j is the junction potential difference across boundary layers,E_D is the Donnan potential difference, R_{ers}, R_b and R_f are the electric resistances of the electrode rinsing solution, C and D bulk solutions and boundary layers respectively, ra and rc are the specific AMV and CMV membrane resistances and ame is the effective electrode surface area as viewed by the electrodes themselves.

Additionally, in 2010 a model was developed in order to represent the transport phenomena and the electrochemical system in the ED batch process for HCl recovery [31]. The Nernst-Planck equation, which is the irreversible thermodynamic approach, was used to describe the ions and water transport inside the ED cell. The Henderson, Kohlrausch, Ohm and Kirchhoff equations were implemented to express the potential drops and resistances in the ED stack. To ensure the equations representing the ED process can be solved and has a unique solution, the degree of freedom (DOF) analysis was carried out. From the analysis, 38 unknown parameters were identiÞed, 27 of which relate to the membrane and the ED stack geometry, the transport properties of the membranes and solution, limiting current index constant and physical properties. The remaining 11 parameters were obtained using various equations. All the models presented in this paper were able to fit the experimental data quite well and they can be employed for use and prediction of batch electrodialysis for HCl recovery. However, the effect of flowrate on process time and energy consumption was found to be insignificant.

In 2011 Petr Cervenka et al. [32] proposed an alternative kinetic description of electrochemical interactions. They presented a one dimensional (1D) mathematical model consisting of the Poisson's equation, the molar balances of chemical components, and the electrochemical reaction kinetics at the electrode surface.

The molar balances of components in the steady state that they used were written in the form of the Nernst-Planck equation. Therefore, they expressed the flux as follows:

$$J_i = -D_i\frac{\partial c_i}{\partial x} - \frac{z_i D_i F}{RT}c_i\frac{\partial \phi}{\partial x} \tag{1.40}$$

And the electric potential (satisfies the Poisson's equation) as:

$$\varepsilon \frac{\partial^2 c_i}{\partial x^2} = -q = -F \sum_i z_i c_i, i = A^+, B^- \tag{1.41}$$

Where q is the electric charge density, E is the electric permittivity of the electrolyte.

To fully define the mathematical problem Petr Cervenka et al. used a series of boundary conditions. This model is useful for dynamic studies despite the fact that it does not contain the electrochemical equilibrium assumption at the electrode/electrolyte interface and a more complex scheme must be suggested.

As we described in a previous section three types of transport phenomena exist in an electrochemical system, diffusion, convection and migration. In 2016 Ghorbani et al. [33] developed a mass transfer model that incorporates all relevant factors; migration, diffusion, and convection to predict ion transfer in electrodialysis cells more completely than conventional models, which neglect convection. Ghorbani et al. used the complete Navier-Stokes equations and Nernst-Planck equations and solved them by the finite difference numerical method in the particular control volumes. The equations in the dilute chamber are numerically solved using techniques from computational fluid dynamics (CFD). In order to evaluate the reliability and accuracy of the model, Ghorbani et al. compared the results with theory as calculated by the NernstÐPlanck equation. They discovered that the developed model is capable of predicting the velocity distribution, separation percent, ion concentration distribution, and electrolyte potential in the chamber, with results that closely align with the theory.

As we can see there are many ways to approach the modeling of the ED process thus there are no models that are widely accepted by the industry to date and it depends also on the setup of the ED process and the application.

1.10 Recovery of short-chain carboxylic acids (SCCAs)

Platform chemicals is a diverse group of chemicals that can be used as the building block-s/structurally close starting materials for the production of different valuable chemicals, including fuel, pharmaceutically important compounds or industrial chemicals. So far, the platform chemical is mostly dominated by petroleum-based platform chemicals as we can see in fig. 1.7 [7]. However, owing to the depletion of petroleum-based raw materials as well as environmental pollution due to the extensive use of such materials, the concept of renewable feedstock-based platform chemical refinery is gaining attention [34].

"The production of organic acids needs innovations to keep up with the development of modern chemical and biochemical industries. Electrodialysis (ED) may be the key innovation" [13].

In 2004 succinic acid was placed on the US Department of Energy's [8] list between the top 12 platform chemicals from biomass with an annual production of between 16,000 and 30,000 tons a year, with an annual growth rate of 10%, expected to reach an annual production of 600,000 tons by 2020 [35]. Lactic acid was placed in the top 30 with an annual production of 800,000 tons with the United States being the largest consumer followed by China and Western Europe. In Fig. 1.8 we can see the highlighted molecules from the report titled "Top Value Added Chemicals from Biomass" from the US Department of Energy. Acetic acid and Formic acid are also highly used chemicals with various applications. Acetic acid's production is estimated at 14.6 M tons p.a. and Formic acid's at 720,000 tons p.a. Additional examples of the main uses of these four SCCAs are given in Tb. 1.1. To date, ED is accepted as an environmentally friendly technique for the recovery of carboxylic acids. As we mentioned before one of the methods for the production of carboxylic acid is fermentation and chemical synthesis. The steps that are included in both methods cannot be considered as environmentally friendly. The efficiency and economics of carboxylic acid production by fermentation and chemical synthesis are still problematic from several points of view [36]. Therefore, current research efforts are focused on identifying effective, efficient, and economic downstream processes to recover carboxylic acids from the fermentation broth.

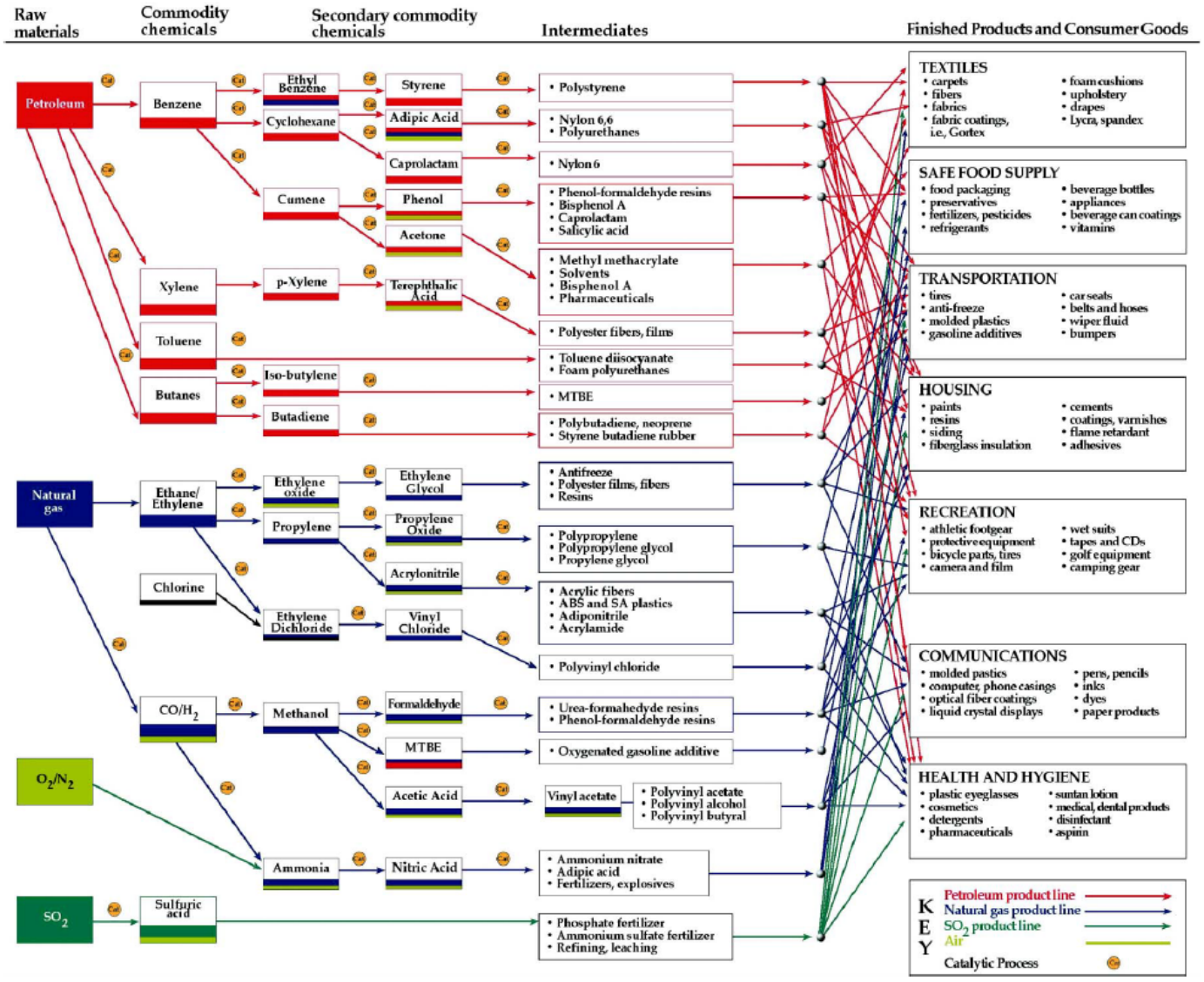

Figure 1.7: Flow-Chart for Products from Petroleum-based Feedstocks (Green, 2012)[7]

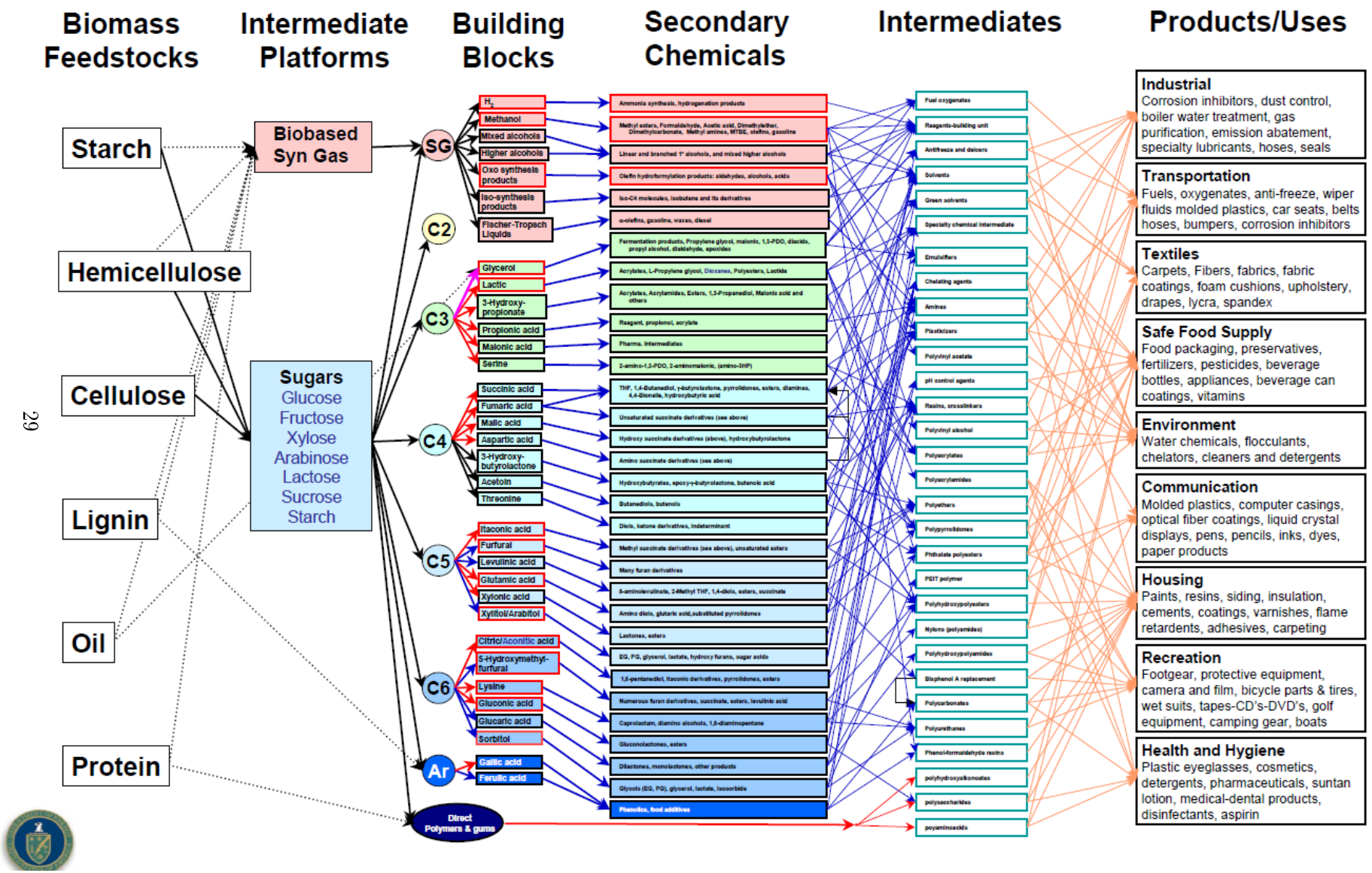

Figure 1.8: Analogous model of a bio-based product flow-chart for biomass feedstocks (Petersen et al., 2010)[8]

Table 1.1: Main applications of acetic, lactic, formic and succinic acid

	Mr (g/mol)	Prod./y	Main Applications	References
Acetic acid	60.05	14.6m	rubber, plastics, acetate fibers, pharmaceuticals, photographic chemicals, food industry	[37], [38]
Formic acid	46.03	720,000	leather production including tanning, rubber production, medical use, cleaning products, use in fuel cells	[37], [38], [39]
Lactic acid	90.08	800,000	biodegradable polymer, food and beverage (flavoring and preservative), personal care and pharmaceutical, textile printing , cosmetics	[24],[37],[38],[40]
Succinic acid	118.9	16,000-40,000	food industry (flavoring and sweetener), pharmaceutical industry, production of resins, coatings, pigment, polyester polyols	[41], [42],[35]

ED as a part of the membrane separation and purification technologies has proven its benefits in the field of recovery and can naturally be considered as one of the strongest environmentally competitive techniques. Energy - related electrodriven membrane processes such as ED are growing rapidly with the help of advanced ion exchange membranes [41]; of course, more research has to be done in order to reduce the cost of electrodialysis even more.

Chapter 2

Materials and Methods

2.1 Introductory experiments

The experimental setup (Fig. 2.1) used to perform the introductory experiments. This layout consist of an electrochemical membrane reactor, divided in two compartments, an anode compartment and a cathode one, divided by an anion exchange membrane. The effective membrane area (Am) was 96.2 cm^2. In each compartment there was an electrode connected to a power supply. Between the membrane and each electrode there was a plastic spacer (Fig. 2.2). Two duran bottles were connected with a stirring system to continuously provide the cell with anolyte and catholyte at a flow rate of 2.99 $L{\cdot}h^{-1}$ in the catholyte and 2.71 $L{\cdot}h^{-1}$ in the anolyte (Appendix II). A power supply (HY6003D, Automation Technology Inc., Hoffman Estates, IL) in galvanostatic mode (constant current) was connected to the cathode (316 L stainless steel mesh, 20 cm tall, 5 cm wide, mesh width: 564 mm , wire thickness: 140 mm, Solana, Schoten, Belgium) and the anode (titanium mesh electrode coated with Ir MMO; 18.8 cm tall, 4.8 cm wide, 0.1 cm thick, Magneto special anodes B.V., Schiedam, The Netherlands), 21 and an Ag/AgCl reference electrode was inserted into the catholyte (alkaline extraction solution). A water bath was used in the duran bottle of the anolyte to prevent the crystallisation of succinic acid, and a magnetic stirrer in the catholyte bottle (Fig. 2.1). Before activating the electrochemical cell, the membrane was immersed for 12 h in NaCl 5%w$\cdot L^{-1}$. The whole system was maintained in room temperature.

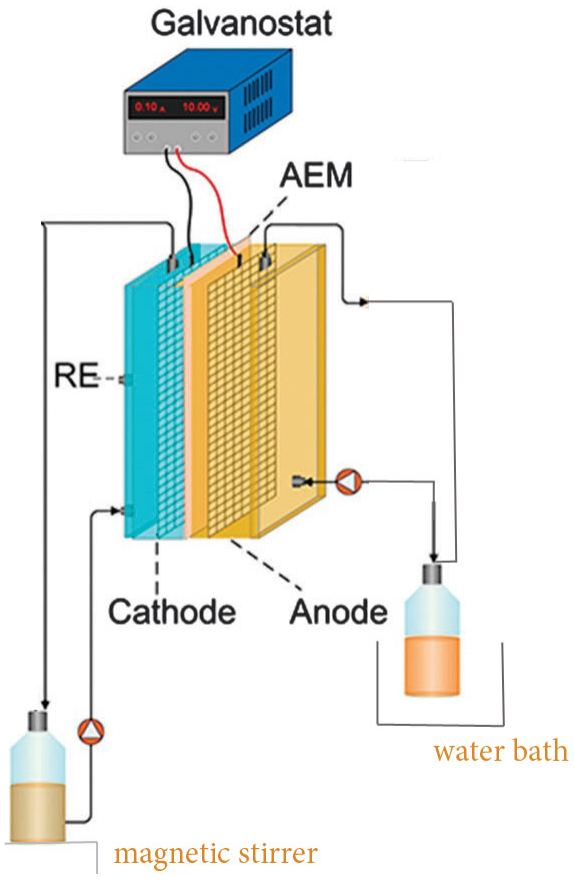

Figure 2.1: Setup of experimental apparatus. (Xu et al.,2015) [2]

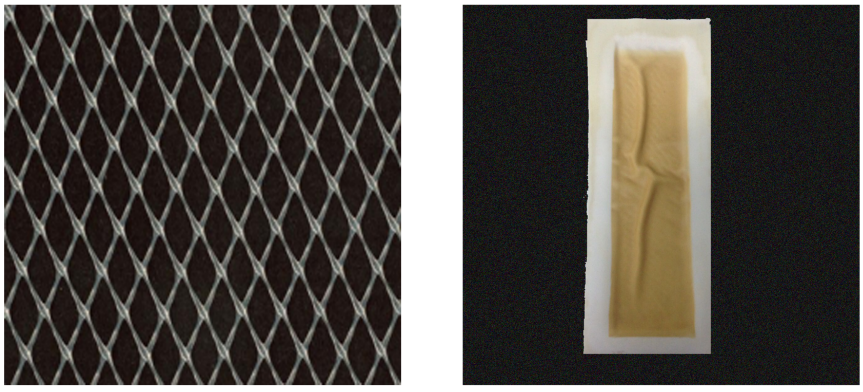

Figure 2.2: Anion-Exchange Membrane (AMI 7001S), Photo of real spacer net (Nemecek M. et al.,2017) [4]

Table 2.1: Physiochemical and electrochemical properties of the anion-exchange membrane

Property	**Value**
Membrane area (cm^2)	96.2
Thickness (mm)	0.45
Total exchange capacity ($meq \cdot g^{-1}$)	31.3
Electrical Resistance ($Ohm \cdot cm^2$)	<40

In the system an Anion-Exchange Membrane (AMI 7001S) (Fig. 2.2)was used, with the following properties(Table 2.1).

In the system, Na_2HPO_4, 10 mM concentration was used at 200 mL volume in the anolyte. whereas in the catholyte there were aqueous solutions of known concentration and volume (500 mL). Twenty two sets of experiments were performed. In the beginning, the experiment took place without electricity and then for concentration of 0.25 M and stable intensity of 0.57 A and 1.12 A and concentration of 0.5 M and stable intensity of 0.57 A and 1.12 A. Subsequently there followed some experiments for the concentrations 0.5 M and 0.25 M and for stable intensity (1.12 A) for lactic acid, formic acid, acetic acid and a mixture with all the solutions mentioned above. During the progress of the experiments the voltage and the density were recorded and there were also pH measurements taken for several points in time.

The organic acids concentrations were determined using a Shimadzu HPLC system using a Shimadzu RI detector and an Aminex HPX-87H (7.8 x 300 mm) column. The temperature of the column was 65 °C and the mobile phase was a 10 mM H_2SO_4 aqueous solution with 0.6 mL/min flow rate. For every set of data we calculated a series of parameters (flux, energy consumption, current efficiency, recovery percentage).

The flux from the catholyte to the anolyte (J), was determined from Eq. (2.1):

$$J = \frac{V_a}{A} \frac{C_t - C_0}{\Delta t} \,, \tag{2.1}$$

where C_t and C_0 are the initial and final concentrations at time t, Δt is the time allowed for the process (h), V_a (m^3) the total volume of of anolyte, and A the effective membrane area (m^2).

The energy consumption and the current efficiency were also determined to evaluate the suitability of the electrochemical process for practical applications.The energy consumption was determined from Eq. (2.2).

$$W_t(\frac{kWh}{kg}) = \frac{V_t \cdot I_t}{w_{t-\Delta t}} \cdot \Delta t, \tag{2.2}$$

where V_t(V) is the applied voltage, I(A) is the current, t(h) is the time, and w(kg) is the weight of the acid in the anolyte.

Current efficiency is the ratio of the electrochemical equivalent current density for a specific reaction to the total applied current density. Current efficiency describes the efficiency

with which charge (electrons) is transferred in a system facilitating an electrochemical reaction. This phenomenon was originally understood through Michael Faraday's work and expressed in his laws of electrolysis.
Current efficiency was determined from Eq. (2.3).

$$n(\%) = \frac{w \cdot z \cdot F}{M \cdot I \cdot t} \times 100 \, , \tag{2.3}$$

where w(mol) is the weight of the acid in the anolyte, F is the Faraday constant (26.8 $\frac{Ah}{mol}$), z is the anion charge, M is the molecular weight, I(A) is the current and t(h) is the time.

Finally in each sample the percentage of the acid was calculated recovery of the product was calculated.

$$Pr.rec.(\%) = (100 - \frac{w_t}{w_0}) \times 100 \, , \tag{2.4}$$

where w_t is the mass formed in the catholyte and w_o the initial mass that we put in the catholyte.

2.2 Prediction model of the concentration values based on the current

Our prediction model we were based on Kohlrausch's laws and we estimated the parameters with the Least Square Method.

1 Least Squares Method [1]

The response variable is linear with the parameters, thus the phenomenon being studied can be described by the following object function:

$$y = \sum_{i=0}^{k} \theta_i x_i = x^T \theta, \tag{2.5}$$

For n experimental data for the independent variables x and the dependent variable y, for every pair of experimental data :

$$y_i = \sum_{i=0}^{k} \theta_i x_{i,j} = \begin{bmatrix} 1 & x_{i,j} & \cdots & x_{k,j} \end{bmatrix} = \begin{bmatrix} \theta_0 \\ \theta_1 \\ \vdots \\ \theta_k \end{bmatrix} = x_j^T \theta, \quad j = 1, 2, ..., n \tag{2.6}$$

or

$$\begin{bmatrix} y_1 \\ y_2 \\ \vdots \\ y_n \end{bmatrix} = \begin{bmatrix} 1 & x_{1,1} & \cdots & x_{k,1} \\ 1 & x_{1,2} & \cdots & x_{k,2} \\ \vdots & \vdots & \ddots & \vdots \\ 1 & x_{1,1} & \cdots & x_{k,n} \end{bmatrix} \cdot \begin{bmatrix} \theta_0 \\ \theta_1 \\ \vdots \\ \theta_k \end{bmatrix} \tag{2.7}$$

and we define the following vectors and matrices

$$\mathbf{y} = \begin{bmatrix} y_1 \\ y_2 \\ \vdots \\ y_n \end{bmatrix}, \mathbf{X} = \begin{bmatrix} 1 & x_{1,1} & \cdots & x_{k,1} \\ 1 & x_{1,2} & \cdots & x_{k,2} \\ \vdots & \vdots & \ddots & \vdots \\ 1 & x_{1,1} & \cdots & x_{k,n} \end{bmatrix} \tag{2.8}$$

thus Eq. (2.7) become

$$\mathbf{y} = \mathbf{X}\boldsymbol{\theta} \tag{2.9}$$

The experimental data contain errors. Thus, even if we study a linear system Eq. (2.7) is not entirely satisfactory and we have to determine the error vector $\boldsymbol{\varepsilon}$

$$\begin{bmatrix} y_1 \\ y_2 \\ \vdots \\ y_n \end{bmatrix} = \begin{bmatrix} 1 & x_{1,1} & \cdots & x_{k,1} \\ 1 & x_{1,2} & \cdots & x_{k,2} \\ \vdots & \vdots & \ddots & \vdots \\ 1 & x_{1,1} & \cdots & x_{k,n} \end{bmatrix} \cdot \begin{bmatrix} \theta_0 \\ \theta_1 \\ \vdots \\ \theta_k \end{bmatrix} + \begin{bmatrix} \varepsilon_0 \\ \varepsilon_1 \\ \vdots \\ \varepsilon_n \end{bmatrix} \tag{2.10}$$

or

$$\mathbf{y} = \mathbf{X}\boldsymbol{\theta} + \boldsymbol{\varepsilon} \tag{2.11}$$

To identify the vector $\boldsymbol{\theta}$, if we have available the n, the amount of the experimental data $(y_j, \mathbf{x}_j^T, j = 1, 2, ..., n)$,we have to calculate the vector $\boldsymbol{\theta}$ that minimizes the scalar variable $\boldsymbol{\varepsilon}^{\boldsymbol{T}}\boldsymbol{\varepsilon}$

The method that estimates the vector $\boldsymbol{\theta}$ is know as least square method or LS method.

$$\boldsymbol{\theta}_{LS} = \{\boldsymbol{\theta} \text{ is the solution to the problem } \min_{\boldsymbol{\theta}} \boldsymbol{\varepsilon}(\boldsymbol{\theta})^T \boldsymbol{\varepsilon}(\boldsymbol{\theta})\} \tag{2.12}$$

To solve this problem we replace Eq. (2.11) and it becomes

Assuming that $\mathbf{y}^T\mathbf{X}\boldsymbol{\theta} = (\boldsymbol{\theta}^T\mathbf{X}^T\mathbf{y})^T$ and the variable $\mathbf{y}^T\mathbf{X}\boldsymbol{\theta}$ is scalar Eq. (**??**) becomes

$$\boldsymbol{\varepsilon}^{\boldsymbol{T}}\boldsymbol{\varepsilon} = \mathbf{y}^T\mathbf{y} - 2\mathbf{y}^T\mathbf{X}\boldsymbol{\theta} + \boldsymbol{\theta}^T\mathbf{X}^T\mathbf{X}\boldsymbol{\theta} \tag{2.13}$$

Subsequently we calculate the slope with respect to the vector $\boldsymbol{\theta}$

$$\frac{d(\boldsymbol{\varepsilon}^{\boldsymbol{T}}\boldsymbol{\varepsilon})}{d\boldsymbol{\theta}} = -2\frac{d(\mathbf{y}^T\mathbf{X}\boldsymbol{\theta})}{d\boldsymbol{\theta}} + \frac{d(\boldsymbol{\theta}^T\mathbf{X}^T\mathbf{X}\boldsymbol{\theta})}{d\boldsymbol{\theta}} = -2\mathbf{X}^T\mathbf{y} + 2\mathbf{X}^T\mathbf{X}\boldsymbol{\theta} \tag{2.14}$$

in writing the last equality we have used the following identities

$$\frac{d(\mathbf{c}^T\mathbf{z})}{d\mathbf{z}} = \mathbf{c}, \frac{d(\mathbf{z}^T\mathbf{A}\mathbf{z})}{d\mathbf{z}} = 2\mathbf{A}\mathbf{z} \tag{2.15}$$

where $\mathbf{c}$, $\mathbf{z}$ are vectors and $\mathbf{A}$ every symmetric matrix. In the most optimized solutions the vector of the gradient should be equal with the zero vector.
Thus,

$$-2\mathbf{X}^T\mathbf{y} + 2\mathbf{X}^T\mathbf{X}\boldsymbol{\theta} = 0 \Rightarrow (\mathbf{X}^T\mathbf{X})\boldsymbol{\theta} = \mathbf{X}^T\mathbf{y} \tag{2.16}$$

or

$$\hat{\boldsymbol{\theta}} = \boldsymbol{\theta}_{LS} = (\mathbf{X}^T\mathbf{X})^{-1}\mathbf{X}^T\mathbf{y} \tag{2.17}$$

For the sum of squared errors (SSE) $\boldsymbol{\varepsilon}^{\boldsymbol{T}}\boldsymbol{\varepsilon}$ we know that

$$SSE = \boldsymbol{\varepsilon}^{\boldsymbol{T}}\boldsymbol{\varepsilon} = \sum_{i=1}^{n}(y_i - \hat{y_i})^2 = \mathbf{y}^T\mathbf{y} - \hat{\boldsymbol{\theta}}^T\mathbf{X}^T\mathbf{y} \tag{2.18}$$

The scalar quantity

$$SST = \sum_{i=1}^{n}(y_i - \bar{y_i})^2 \tag{2.19}$$

it is called total sum of squares and is the sum of the squares of the deviations of all the experimental points of the independent variable from their mean. Using the identity

$$\underbrace{\sum_{i=1}^{n}(y_i - \bar{y_i})^2}_{\text{SST}} = \underbrace{\sum_{i=1}^{n}(y_i - \hat{y_i})^2}_{\text{SSE}} + \sum_{i=1}^{n}(\hat{y_i} - \bar{y_i})^2 \tag{2.20}$$

we assume that the total coefficient of variation (SST) consists of the coefficient of variation that can not be explained based on the current model (SSE) and an additional term which is the term of dispersion that explains the current model

$$SSR = \sum_{i=1}^{n}(\hat{y_i} - \bar{y_i})^2 \tag{2.21}$$

thus,

$$SST = SSE + SSR \tag{2.22}$$

From Eq. (2.19)

If this value is bigger than the statistically significant result α we do not reject the hypothesis $\theta_i = \theta_i^*$.

2.3 Dynamic model

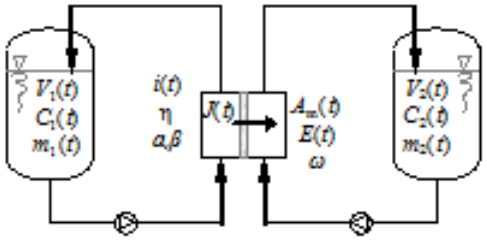

Figure 2.3: Schematic diagram of electrodialysis

The system of differential equations has been solved using Matlab (Appendices III & IV) and the parameters were estimated with the least square method as we have described earlier in Section 2.2 . The simulation results are compared with the experimental results.

The rate of anion transfer is proportional to the current applied:

$$\frac{d(V_1C_1)}{dt} = -J \tag{2.23}$$

$$\frac{d(V_2C_2)}{dt} = +J \tag{2.24}$$

where:

$$J = \eta(\frac{iA_m}{zF}) \tag{2.25}$$

where C_1 is the acid concentration in the catholyte compartment, C_2 the concentration of acid in the anolyte compartment, V_1 the volume of the catholyte compartment, V_2 the volume of the anolyte compartment, η the current efficiency, i the current density, z the charge of the ion, (for succinic acid z=2, $z = 1$ for acetic, lactic and formic acid), A_m the membrane active area, J the molar flow of the acid through the membrane and F the the Faraday constant.

The volume of the catholyte compartment can be determined by:

$$\frac{d(V_1)}{dt} = -J \cdot (\frac{1}{\rho_w} + \frac{\omega}{\rho_{sa}}) \tag{2.26}$$

and the volume of the anolyte compartment by:

$$\frac{d(V_2)}{dt} = +J \cdot (\frac{1}{\rho_w} + \frac{\omega}{\rho_{sa}}) \tag{2.27}$$

where ω is the electroosmosis coefficient of water, ρ_w the density of water and ρ_{sa} the density of the acid.

The voltage across the membrane module can be determined by:

$$V = IR \tag{2.28}$$

where R is the resistance of the membrane:

$$R = \alpha + \frac{\beta}{C^n} \tag{2.29}$$

where α and β are the constants in the combined resistance model that we descriped in Chapter 3 and n=0.5.

The mass of the acid in the catholyte compartment can be determined by:

$$m_1 = MWV_1C_1 \tag{2.30}$$

and the mass of the acid in the anolyte compartment by:

$$m_2 = MWV_2C_2 \tag{2.31}$$

where MW is the molecular weight of the acid.

The power consumption can be determined by:

$$P = I^2R \tag{2.32}$$

Chapter 3

Results & Discussion

In the following sections the results for eight sets of experiments are presented. Three with succinic acid, one without the presence of electric field and two at 0.25 M and 0.5 M concentrations and a constant current of 0.57 A. Three experiments at 0.25 M concentration and at constant current (0.57 A) with lactic acid, formic acid and acetic acid, and two experiments at 0.25 M and 0.5 M concentrations and a constant current of 1.12 A for a mixture with all the aformentioned acids.

3.1 Effect on ion transport in the absence of electric current

Electric current was not applied in order to observe ion transport through the ion selective membrane. The catholyte consisted of a succinic acid aqueous solution 0.25 M of 500 mL volume and the anolyte consisted of 200 mL of Na_2HPO_4 10 mM concentration. Samples were taken for 24 h (Table A.1).

The concentrations showed that a negligible quantity of succinic acid was transferred from the anolyte to catholyte as we expected. At 8h of the process about 3.6% and at 24h about 4.5% recovery of succinic acid was achieved.

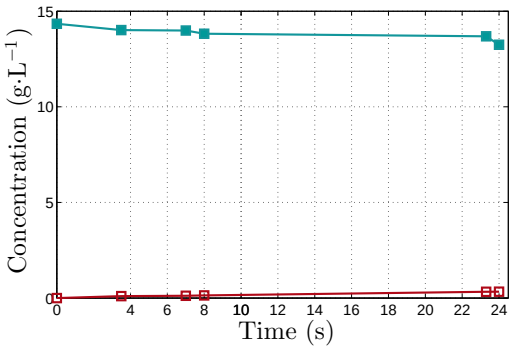

Figure 3.1: Succinic acid concentration in the anolyte and the catholyte versus time for 0.25 M, catholyte (■), anolyte (□)

3.2 Effect of ion transport in the presence of electric current

1 Ion trasport of short-chain carboxylic acids (SCCAs)

In order to select the initial concentration of the acids, we conducted two experiments with two different concentrations of succinic acid 0.25 M and 0.5 M. The current applied was 0.57 A. Initially, the catholyte consisted of succinic acid aqueous solution 0.25 M and 0.5 M of 500 mL volume and 200 mL of Na_2HPO_4 10 mM concentration in the anolyte. Measurements were taken for 10 h (Table A.2 and Table A.3). For around 10 h about 55% and 93.3% of the succinic acid 0.5 M and 0.25 M, respectively had passed into the anolyte (Fig. 3.2 and Fig. 3.3).

We observed that the value of energy consumption was in between 4.8 - 6.3 kWh/kg and 5.28 - 5.55 kWh/kg for succinic acid 0.25 M and succinic acid 0.5 M, respectively (Fig. 3.6, Fig. 3.7). Additionally, the power consumption for succinic acid 0.25 M and 0.5 M was in between 3.9 - 13.0 KW and 5.2 - 5.8 KW, respectively (Fig. 3.14, Fig. 3.5).

The initial energy and power consumption were lower at 0.5 M of succinic acid than 0.25 M and the flux of succinic acid 0.25 M was higher than 0.5 M concentration (Fig. 3.4 and in Fig. 3.9). Finally taking into consideration the fact that the recovery at 0.25 M was higher than 0.5 M, the following experiments were performed at 0.25 M initial concentartion. The reason to apply a 0.57 A current was that at 1.12 A, high voltage limits were reached (30.1 V) at a very early stage of the experiment which could lead to misleading conclusions. As the experiments progressed, anions were transferred from the catholyte to the anolyte, and simultaneously H^+ was formed through water splitting and the oxidation of oxygen. These processes led to an increase in the concentration in the anolyte with time and, thus, to a simultaneous increase in the potential of the system at constant applied current. The electrical resistance of the catholyte also decreased with time because of the formation of highly conductive OH^- at the cathode as literature indicates ([24], [9]). In order to reduce those high amounts of resistance and conductivity we investigated the relation between the current through our membrane and the simultaneous voltage drop across membrane and solution boundary layers by determining the so-called current - voltage curves but the

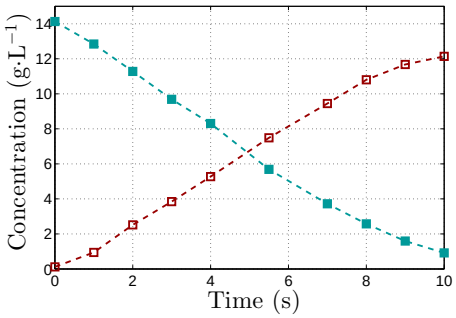

Figure 3.2: Succinic acid concentration in the anolyte and the catholyte versus time for 0.25 M 0.57 A 10 h, catholyte (■), anolyte (□)

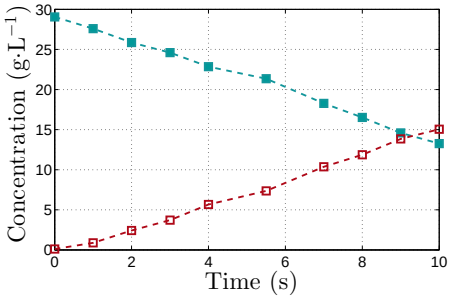

Figure 3.3: Succinic acid concentration in the anolyte and the catholyte versus time for 0.5 M 0.57 A 10 h, catholyte (■), anolyte (□)

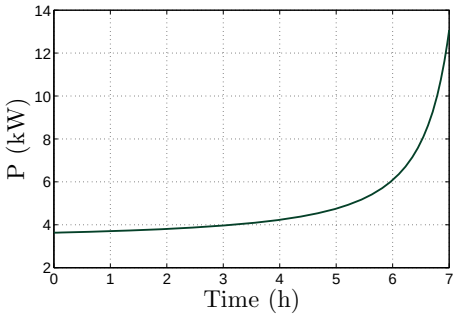

Figure 3.4: Power consumption versus time for succinic acid 0.25 M

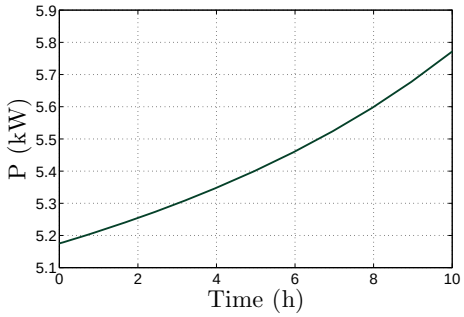

Figure 3.5: Power consumption Versus time for succinic acid 0.5 M

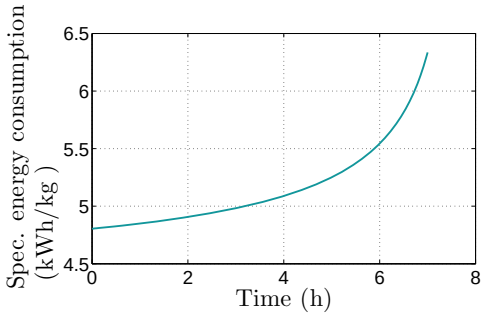

Figure 3.6: Spec. energy consumption Versus time for succinic acid 0.25 M

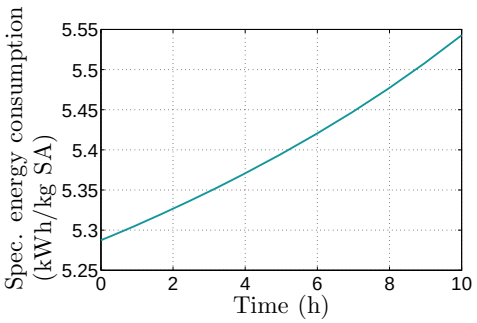

Figure 3.7: Spec. energy consumption Versus time for succinic acid 0.5 M

extraction of efficient conclusions was not possible as we can see in Appendix B.

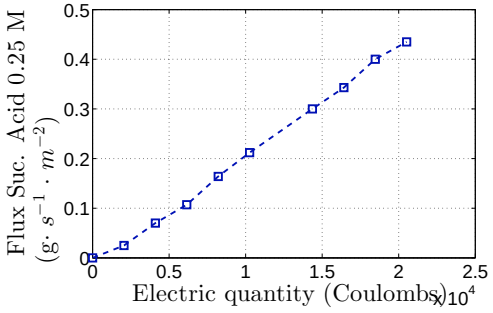

Figure 3.8: Variation of succinic acid 0.25 M flux in the catholyte at 0.57A for 10h process

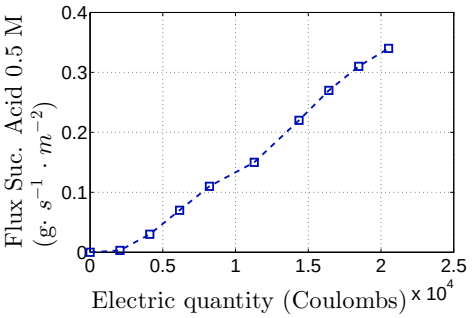

Figure 3.9: Variation of succinic acid 0.5 M flux in the catholyte at 0.57A for 10h process

2 Recovery of short-chain carboxylic acids (SCCAs)

In this set of experiments 500 mL of aqueous solution of SCCAs 0.25 M concentration were added in the catholyte and 200 mL of Na_2HPO_4 10 mM in the anolyte. The constant current imposed was 0.57 A. Measurements were taken for 6 - 10 h. The time of the process was voltage- dependent by the equipment's upper (voltage) limits as it shown in Tables: A.2, A.4, A.5, A.6.

We observed that at 6 h of process about 93.6% of the acetic acid had passed in the anolyte, at 7 h about 90.6% of the formic acid, at 8 h about 96.7% of lactic acid and at 10 h 93.4% of the succinic acid (Fig. 3.10-Fig. 3.13).

In Fig. 3.14, Fig. 3.15, Fig. 3.16 and in Fig. 3.17 the dependency of the energy consumption is presented. We observed that for succinic acid the energy consumption was between 4.8 - 6.3 kWh/kg, for acetic acid between 8.26 - 10.84 kWh/kg, for lactic acid between 4.58 - 8.75 kWh/kg and for formic acid between 4.8 - 6.3 kWh/kg. Similar en-

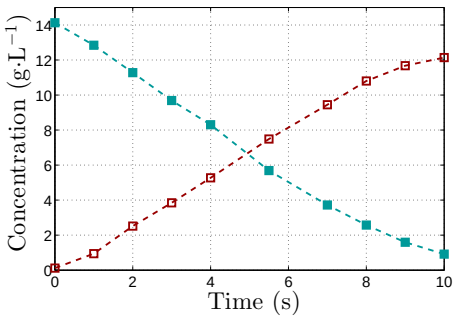

Figure 3.10: Succinic acid concentration in the anolyte and the catholyte versus time for 0.25 M 0.57 A 10 h, catholyte (■), anolyte (□)

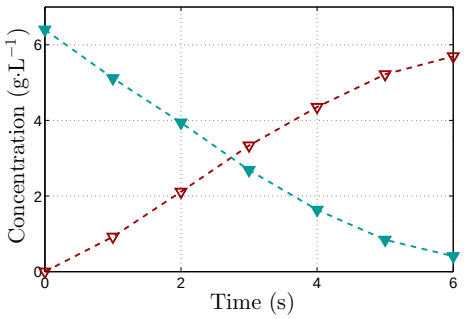

Figure 3.11: Acetic acid concentration in the anolyte and the catholyte versus time for 0.25 M 0.57 A 6 h, catholyte (▼), anolyte (▽)

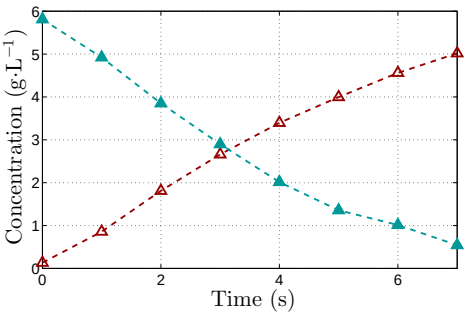

Figure 3.12: Formic acid concentration in the anolyte and the catholyte versus time for 0.25 M 0.57 A 7 h, catholyte (▲), anolyte (△)

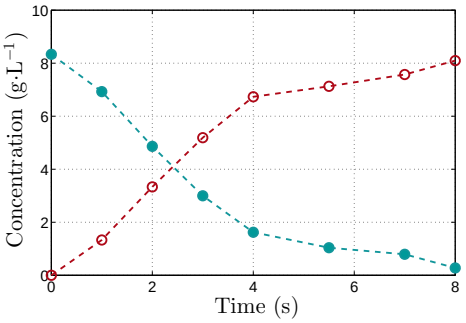

Figure 3.13: Lactic acid concentration in the anolyte and the catholyte versus time for 0.25 M 0.57 A 8 h, catholyte (●), anolyte (○)

ergy requirements of 0.91-8.02 kWh/kg have been achieved in other studies for small and medium chain carboxylic acid production [2].

Additionally, in Fig. 3.18, Fig. 3.19, Fig. 3.20 and in Fig. 3.21 the dependency of the power consumption is presented. We observed that for succinic acid the power consumtion was between 3.9 - 13.0 KW for acetic acid between 8.1 kW - 19 kW, for lactic acid between 5.8 kW - 12.0 kW and for formic acid between 3.8 kWh - 13.0 kW. In Table3.1 we can observe the concentrations in the anolyte and the catholyte for all acids for $\backsimeq 80\%$ recovery. Recovery rates for ED typically exceed 85% and they can be as high as 94% percent [43].

Additionally, in Table 3.1 we presented the current efficiency persentage for each acid. Generally, in most electrodriven processes the overall current efficiency increases until a maximum value is reached. In the ED process, there is an electrical resistance from electrode reactions, water transfer, and protons leakage, so that the overall current efficiency is less than 100% under low concentration and in higher concentrations is more than 100% as we observed with the succinic acid 0.5M. That indicates that the total current applied to the membrane is effectively transferring ions, especially for succinic acid. The remaining of the current can be attributed to loss resulting from cross leakage and back diffusion.

State of the art in the excisting literature is dealing with ED techniques for the recovery of carboxylic acids. Ferrer et al. [39] studied the recovery of formic acid from diluted

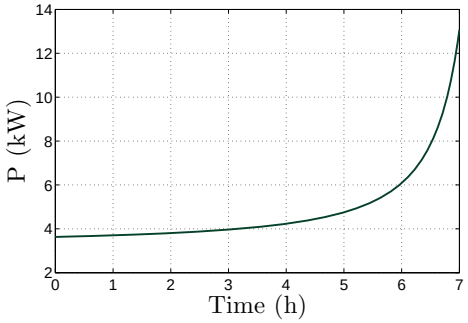

Figure 3.14: Power consumption versus time for succinic acid 0.25 M

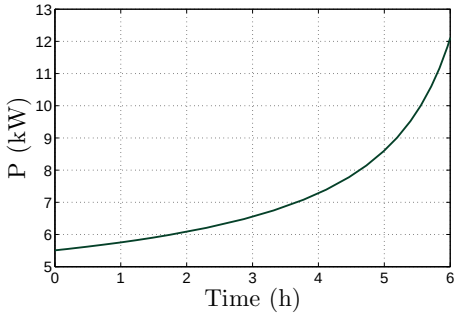

Figure 3.15: Power consumption versus time for lactic acid 0.25 M

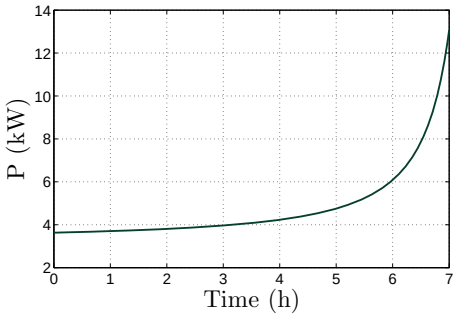

Figure 3.16: Power consumption versus time for formic acid 0.25 M

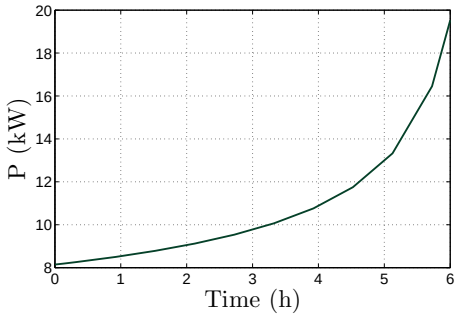

Figure 3.17: Power consumption versus time for acetic acid 0.25 M

sodium formate aqueous solution. The recovery of formic acid was 32%, the current efficiency around 80% under a current density of 0.5 A dm^{-2} and the energy consumption was 2.6 $KWhKg^{-1}$.

By using a two-compartment electro-electrodialysis (EED) cell divided by an anionic membrane, Wang et al. [44] studied the recovery of organic acids like butyric, valeric and adipic acid. The current efficiency was between 20.86-42.14% and the energy consumption was between 3.92 - 22.84 $KWhKg^{-1}$.

The recovery of sodium lactate from model solutions by ED was studied by Fidaleo and Moresi [30], energy consumption was between 0.14 - 0.31 $KWhKg^{-1}$ for a solute recovery yield of 95% and the current efficiency was about 88%.

Saxena et al. [24] developed an electrochemical membrane reactor based on an in-house-prepared anion-exchange membrane to achieve single-step separation and acidification (ion substitution) of lactates to lactic acid. The energy consumption and current efficiency values for the recovery and ion substitution of LaNa from concentrated fermentation broth were observed to be about 5.02 kWh/kg and 47.64%, respectively, for a completely optimized experiment.

Additionally, Xu et al. [2] tested a novel approach to separate medium-chain carboxylic acids (MCCAs), the current efficiency was 53.9% at a current of 10 Am^2 a minimum power consumption of 4.08 ± 0.66 $KWhKg^{-1}$ was achieved.

Comparing our results (Table 3.1) with the aforementioned literature, we observed that we were able to achieve higher recovery and current efficiency percentages. Our energy consumptions levels were higher. The fact that these energy consumption values are at a higher level than those reported indicates the need to develop a more efficient anion exchange membrane with low resistance and high selectivity to reduce energy consumption and enhance current efficiency of the process. Additionally, in many ED processes the actual energy consumption is substantially higher than the theoritical values due to concentration polarisation (Section 1.4) [45].

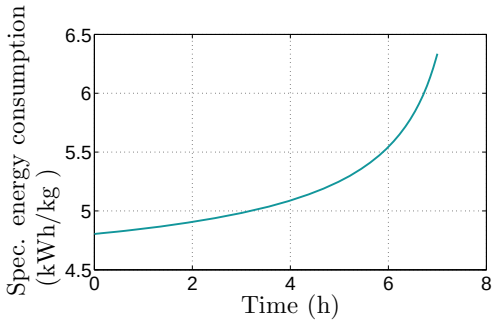

Figure 3.18: Spec. energy consumption versus time for succinic acid 0.25 M

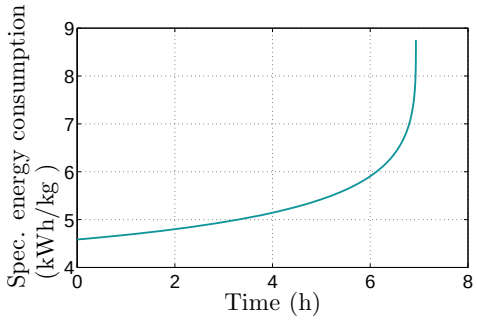

Figure 3.19: Spec. energy consumption versus time for lactic acid 0.25 M

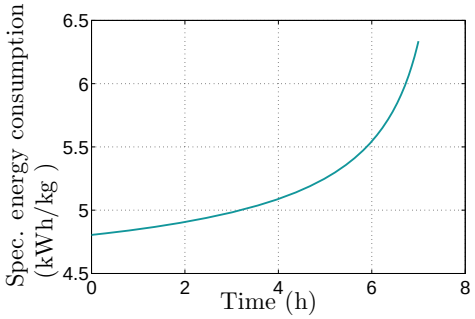

Figure 3.20: Spec. energy consumption versus time for formic acid 0.25 M

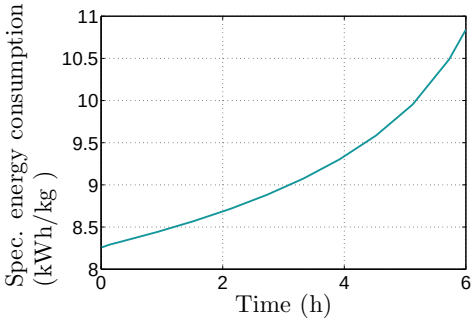

Figure 3.21: Spec. energy consumption versus time for acetic acid 0.25 M

Table 3.1: Concentration in the catholyte and the anolyte, current efficiency, energy concumption, recovery percentage

SCCA	**Process time(h)**	**Acid in the catholyte(g)**	**Acid in the anolyte (g)**	**CE(%)**	**energy consumption**	**Recovery(%)**
succinic acid 0,25M	7	3,7	9,4	95,3	5,7	81
acetic acid	5	0,8	5,2	81	9,8	86
formic acid	6	1	4,6	75	5,5	82
lactic acid	4	0,8	7,6	87,8	5,2	81

3 Ion transport of short-chain carboxylic acids (SCCAs) mixture

In order to investigate if the recovery of SCCAs from mixture solutions have the same rate from those with aqueous solutions we performed a set of experiments. In these experiments 500 mL of aqueous solution of a mixture of succinic acid, acetic acid, lactic acid and formic acid 0.25 M and 0.5M was added in the catholyte and 200 mL of Na_2HPO_4 10 mM in the anolyte. The constant current imposed was 1.12 A. Measurements were taken for 8 h and 12 h respectively, as it shown in Tables A.7 and A.8. In Figs. 3.22, 3.24 and Figs. 3.23, 3.25 the experimental data for the concentrations in the catholyte and in the anolyte were presented respectively for each concentration.

It is observed that for the 0.25 M concentration and for about 8 h, 93.2% of succinic acid, 93.3% of lactic acid, 98.1% of formic acid and 93.3% of acetic acid had passed into the anolyte. And at 0.5 M at 12 h concentration 61.0% of succinic acid, 60.9% of lactic acid, 94.5 % of formic acid and 24.4 % of acetic acid had passed into the anolyte.

Finally the experimental data from the acid solution mixture with those with the aqueous solutions were compared. In Fig. 3.26-3.29 the results for each acid were presented

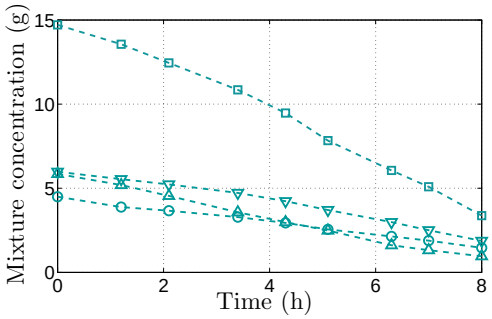

Figure 3.22: Mixture concentration in the catholyte for 0.25 M, 1.12 A, succinic (□), lactic (o), acetic (▽), formic (△)

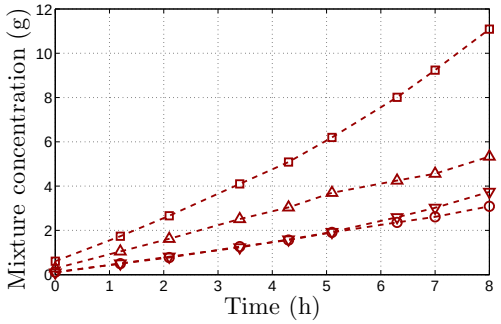

Figure 3.23: Mixture concentration in the anolyte for 0.25 M, 1.12 A, succinic (□), lactic (o), acetic (▽), formic (△)

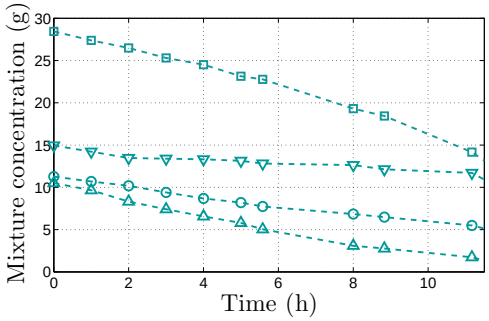

Figure 3.24: Mixture concentration in the catholyte for 0.5 M, 1.12 A, succinic (□), lactic (o), acetic (▽), formic (△)

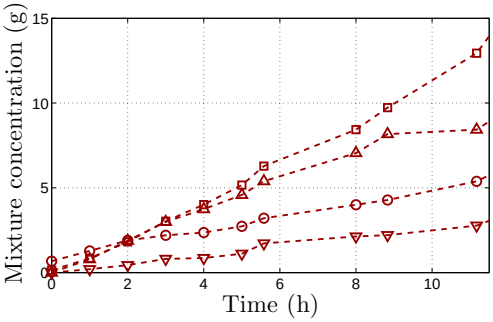

Figure 3.25: Mixture concentration in the anolyte for 0.5 M, 1.12 A, succinic (□), lactic (o), acetic (▽), formic (△)

and in Tb. 3.2 we compared the recovery percentages for 8 h. We observed that the recovery percentage of all acids exclude from the ones of clean aqueous solutions. More precisely, at 8 h the recovery percentage of succinic acid 0.25 M concentration in the clear aqueous solution and in the mixture was 93.2% and 77.1%, respectively and at 12 h the recovery percentage of the mixture was 96.3% as much as in the clear aqueous solution in 8 hours (Fig. 3.26). The recovery percentage for acetic acid was for 8 h 93.3% in aqueous solution versus 83.3% in the mixture and at 12 h the recovery percentage of the mixture was 94.3% (Fig. 3.27). For lactic acid aqueous solution at 8 h the recovery percentage was 93.3% and for the mixture solution 67.5% and 95.2% in the mixture at 8 h and 12 h,respectively. Additionally the recovery percentage difference for formic acid was less than 15% between aqueous solution and mixture and at 12 h the recovery percentage of the mixture was more than 97% (Fig. 3.28). Finally we observed that the concentrations of the SCCAs at the acid mixture solution didn't followed the same linear relationship with time as the ones in clear aqueous solutions but this can also be due to experimental error measurements. Glassner et al. [46] in 1995 studied the recovery of succinic acid and acetic acid from fermentation broth *via* CED with similar results as in this thesis. The recovery percentages for succinic acid and acetic acid were more than 80% and 50%, respectively and the current efficiency was more than 78%.

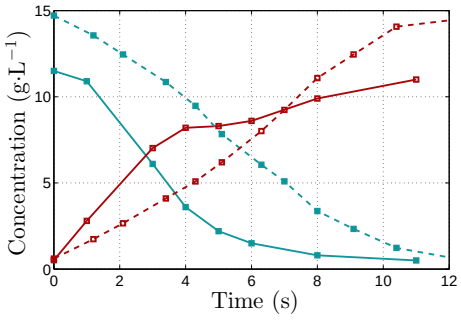

Figure 3.26: Concentration of succinic acid and mixture concentration in the anolyte and the catholyte versus time for 0.25 M, 1.12 A, catholyte (■), anolyte (□)

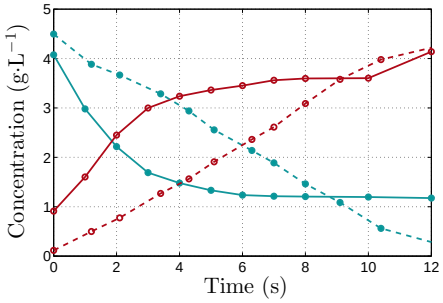

Figure 3.27: Concentration of lactic acid and mixture concentration in the anolyte and the catholyte versus time for 0.25 M, 1.12 A, catholyte (●), anolyte (○)

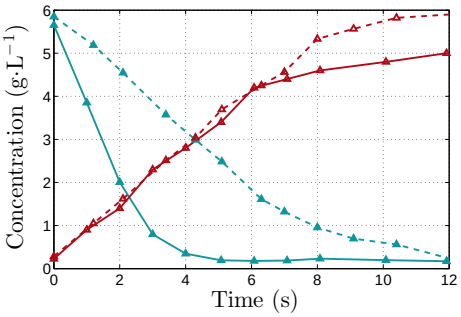

Figure 3.28: Concentration of formic acid and mixture concentration in the anolyte and the catholyte versus time for 0.25 M, 1.12 A, catholyte (▲), anolyte (△)

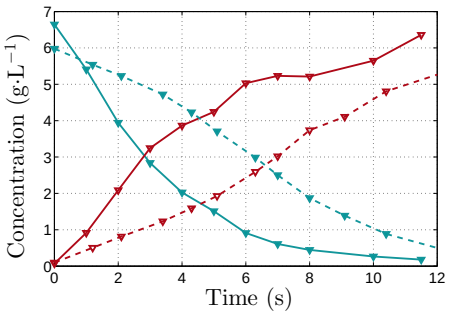

Figure 3.29: Concentration of acetic acid and mixture concentration in the anolyte and the catholyte versus time for 0.25 M, 1.12 A, catholyte (▼), anolyte (▽)

Table 3.2: Recovery percentage for clear and mixture solutions

	Succinic acid	**Lactic acid**	**Formic acid**	**Acetic acid**
recovery % clear solutions	93.2	93.3	98.1	93.3
recovery % mixture	77.1	67.5	83.6	68.8

4 Acids fluxes and influence of the concentration

The acids' fluxes are presented in Fig. 3.30 - Fig. 3.33 for succinic acid, lactic acid, formic acid and acetic acid, respectively. We observed that for every acid the J values have a linear relationship to the electric quantity through the membrane cell. The effects of the acids concentration in the catholyte are presented in Fig. 3.34, were we plotted the fluxes for two different concentrations for succinic acid. The J value increased for higher concentration. Additionally in Fig. 3.35 we presented the maximum values of the flux for each SCCA. As we can see succinic acid had the maximum flux of 0.34 $g{\cdot}s^{-1}{\cdot}m^{-2}$, followed by lactic acid with a maximum flux of 0.23 $g{\cdot}s^{-1}{\cdot}m^{-2}$ and acetic and formic acid with maximum fluxes of 0.16 $g{\cdot}s^{-1}{\cdot}m^{-2}$ and 0.14 $g{\cdot}s^{-1}{\cdot}m^{-2}$, respectively. Comparing our results with the existing literature we observed that we were able to obtain much higher values of flux. Xu et al. ([2]) for the separation of medium-chain carboxylic acids (MCCAs) achieved a maximum flux of 244 $\pm$ 15.7 $g{\cdot}d^{-1}{\cdot}m^{-2}$ and Saxena et al. for the separation of lactates to lactic acid studied the dependency of the flux of lactate (J) from the applied potential gradient and the initial concentration of La^{-} in the anolyte, and they calculated the flux for a constant current of 1 A, between 1.5 - 5.5 10^{-10} $mol{\cdot}s^{-1}{\cdot}m^{-2}$. Finally, for the recovery of pyruvic acid from fermentation broth and for higher voltage values, Zelic and Vasic-Racki ([47]) were able to reach a pyruvatic flux of 367 $g{\cdot}h^{-1}{\cdot}m^{-2}$.

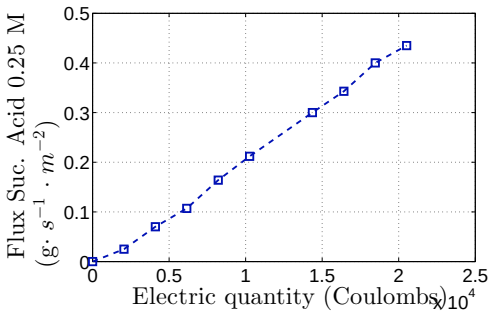

Figure 3.30: Variation of succinic acid flux in the catholyte at 0.57 A for 10 h process

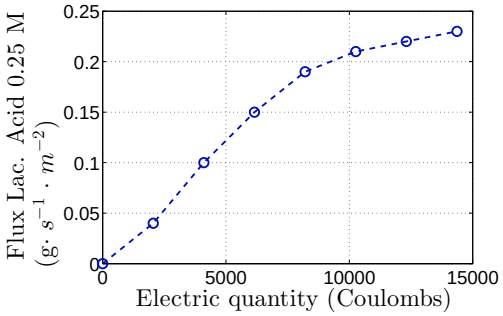

Figure 3.31: Variation of lactic acid flux in the catholyte at 0.57 A for 7 h process

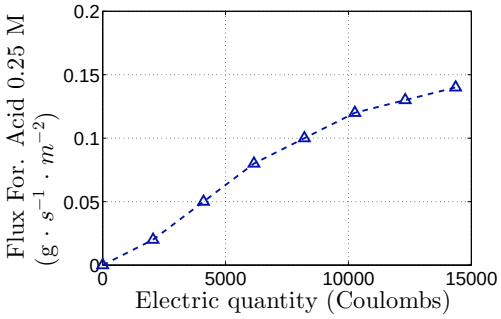

Figure 3.32: Variation of formic acid flux in the catholyte at 0.57A for 7h process

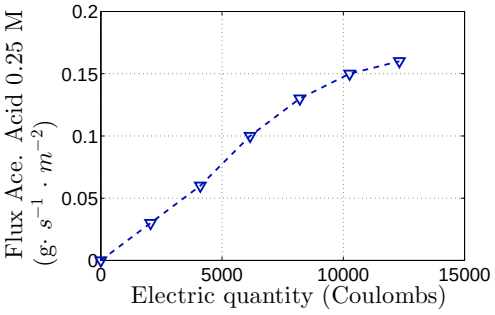

Figure 3.33: Variation of acetic acid flux in the catholyte at 0.57A for 6h process

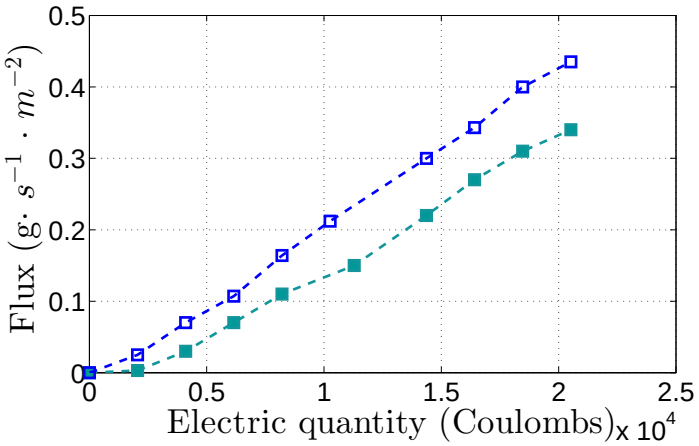

Figure 3.34: Dependence of succinic acid flux on electric quantity (0.57A) at different concentrations for 10h process, succinic acid 0.25 M (■), succinic acid 0.5 M (□)

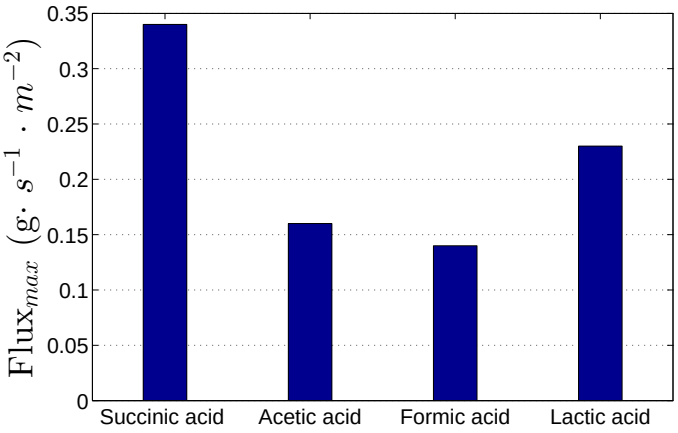

Figure 3.35: Maximum Fluxes of SSCAs

3.3 Prediction model of the concentration values based on the current

As we described in Section 1.7, dilute solutions follow Kohlrausch's Law of concentration dependence and additivity of ionic contributions. The resistance of an electrolyte is normally referred to as conductance and this is $\frac{1}{R}$ where R is the specific resistance. The conductance of an electrolyte is dependent on the ability of the electrolyte to carry a current and this, in turn, is dependent on the degree of dissociation of the electrolyte. The greater the dissociation, the better the conductance. When reffering to the equivalent conductance of an electrolyte, we mean the conductivity of 1 g of equivalent weight of the electrolyte. Hence, the equivalent conductance of the electrolyte will only be half the molecular conductance because the "equivalent" of a bivalent system is half the "molecular". However, it has been shown that the conductance of an electrolyte (R) is dependent on the equivalent conductance at infinite dilution (α) and the concentration of the electrolyte (C) and an experimental constant (k), thus:$R = \alpha - k\sqrt{C}$. Hence conductance is proportional to $\sqrt{C}$, therefore resistance will be proportional to $\frac{1}{\sqrt{C}}$.

Here follow the diagrams (Fig. 3.36-Fig. 3.39) of the resistance $R = \frac{V}{I}$ versus $\frac{1}{C^n}$ for the experiments we performed, in which the abscind is the resistance of the membrane (α) and the slope is the resistance of the solution(k). Therefore knowing the resistance we can predict the concentration of the acid in the catholyte.

The objective is to estimate the parameters (n,α,k) of the model as we have already described in Section 2.2 with the LSM method, based on the observed pairs of values. In Appendix II is the Mathworks Matlab code used for the estimation of the parameters. The code is comprised of one .m file. Additionally by optimising the total coefficient of variations based on Eq. 2.22 as we can see in Tb. 3.3 we modified Kohlrausch's equation by changing the value of the square roote in the denominator accordingly to the best value of the total variation. A perfect fit would result in an R^2 of 1, a very good fit is when R^2 is near 1 and a very poor fit is when R^2 is near 0. As we can see our results have a very good fit. Thus, the following empirical equations came up:

For succinic acid :

$$R = 10.1937 + \frac{4.3030}{C^{0.29}} \ . \tag{3.1}$$

For acetic acid:

$$R = 10.1415 + \frac{7.2168}{C^{0.47}} \ . \tag{3.2}$$

For formic acid:

$$R = 10.1265 + \frac{0.1523}{C^{1.4}} \ . \tag{3.3}$$

For lactic acid:

$$R = 10.2550 + \frac{2.0560}{C^{0.7}} \ . \tag{3.4}$$

Those equations describe really well the production of the four carboxylic acids as we observed when we compared them with the experimental data (Fig. 3.36-Fig. 3.39). Thus, those equations can be very useful in future experiments as a guide in order to predict the concentrations of SCCAs in the anolyte.

Table 3.3: Model parameters

	α	k	R^2
succinic acid	10.1937	4.3030	0.9528
acetic acid	10.1415	7.2168	0.9790
formic acid	10.1265	0.1523	0.9704
lactic acid	10.2550	2.0560	0.9407

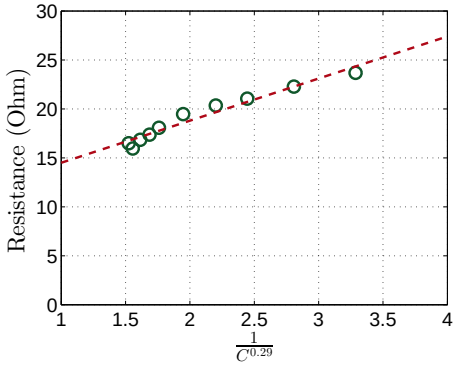

Figure 3.36: Resistance versus $\frac{1}{\sqrt{C}}$ for suc.acid 0.25M 0.57A

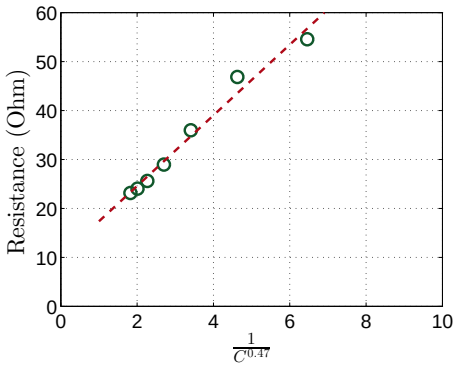

Figure 3.37: Resistance versus $\frac{1}{C^{0.2}}$ for acetic acid 0.25M 0.57A

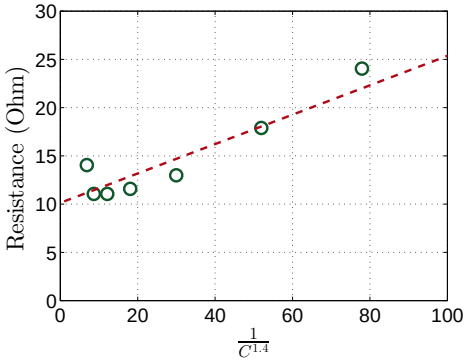

Figure 3.38: Resistance versus $\frac{1}{C^{0.7}}$ for formic acid 0.25M 0.57A

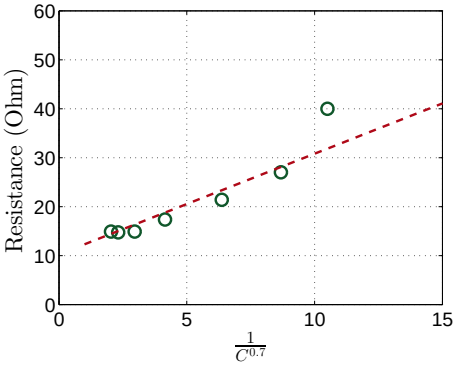

Figure 3.39: Resistance versus $\frac{1}{\sqrt{C}}$ for lactic acid

Chapter 4

Dynamic model

Based on the rationale of the dynamic model presented in Section 2.3 and the calculation of the parameters described in Section 2.2, the prediction for the SCCAs concentrations in the anolyte and in the catholyte are presented in Figures 4.1 - 4.4, the prediction for the volumes in Figures 4.5 - 4.8 and the predictions for the voltage in Figures 4.9 - 4.12. All results are compared with the experimental data and in Appendix II is the Mathworks Matlab code used comprised in one .m file.

The electrodialytic recovery of succinic acid from aqueous solutions (Fig. 4.1) appeared to be quite well simulated using the mathematical model outlined here, together with the parameters determined *via* a series of independent experimental trials. Additionally, for formic acid the recovery seemed to be well simulated despite, lactic and acetic acid who seemed to have small deviations fron the experimental data.

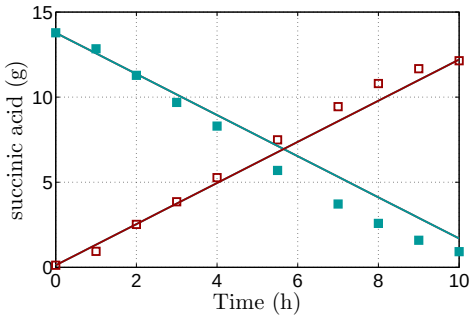

Figure 4.1: Succinic acid concentration in the anolyte and the catholyte versus time for 0.25 M 0.57 A, catholyte (■), anolyte (□)

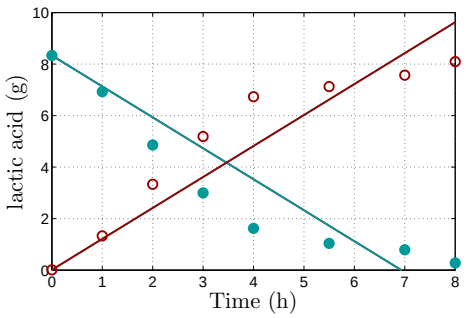

Figure 4.2: Lactic acid concentration in the anolyte and the catholyte versus time for 0.25 M 0.57 A, catholyte (●), anolyte (○)

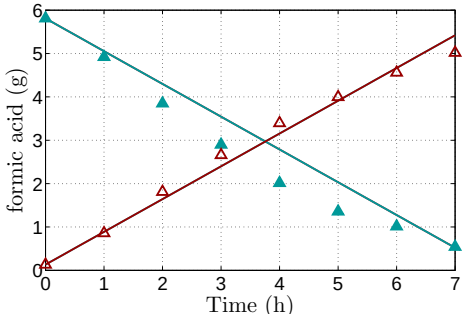

Figure 4.3: Formic acid concentration in the anolyte and the catholyte versus time for 0.25 M 0.57 A, catholyte (▲), anolyte (△)

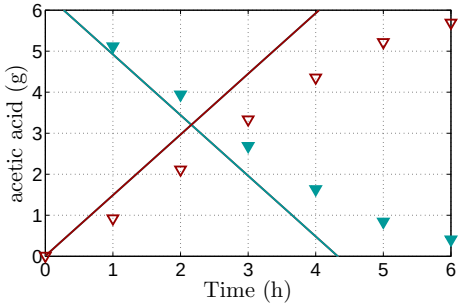

Figure 4.4: Acetic acid concentration in the anolyte and the catholyte versus time for 0.25 M 0.57 A, catholyte (▼), anolyte (▽)

The prediction for the volumes appeared to be quite well simulated with the experimental data as we can in Figures 4.5 - 4.8. For the voltage predictions as we can see for succinic, lactic and formic acid in Fig. 4.9,4.10,4.11, respectively the experimental data seem to fit quite well. For acetic acid (Fig. 4.12) we can observe deviations in voltage prediction, with lower voltage values in the expeimental data. Those discrepancies might be due to problems in operation rather than in modeling. These predictions, for the concentrations in the anolyte and in the catholyte, for volumes and voltage were able to fit the experimental data quite well despite some small deviations and they can be employed for the prediction of carboxylic acid's recovery *via* ED.

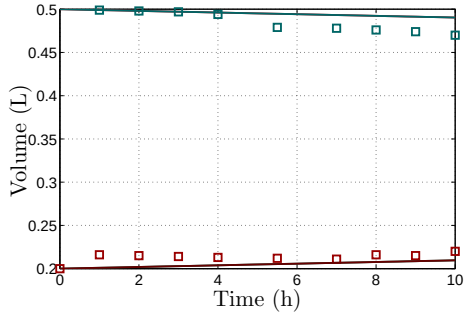

Figure 4.5: Succinic acid volumes in the anolyte and the catholyte versus time for 0.25 M 0.57 A, catholyte(□), anolyte(□)

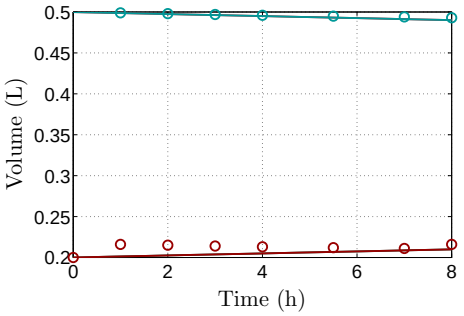

Figure 4.6: Lactic acid volumes in the anolyte and the catholyte versus time for 0.25 M 0.57 A, catholyte (○), anolyte (○)

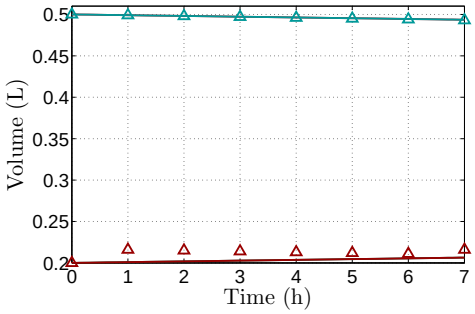

Figure 4.7: Formic acid volume in the anolyte and the catholyte versus time for 0.25 M 0.57 A, catholyte (△), anolyte (△)

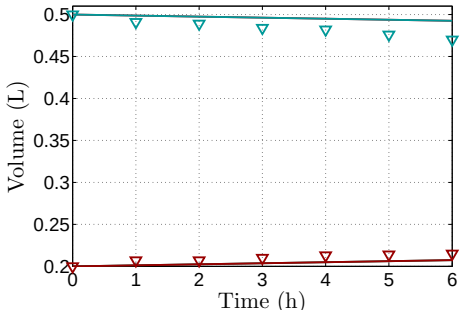

Figure 4.8: Acetic acid volumes in the anolyte and the catholyte versus time for 0.25 M 0.57 A, catholyte (▽), anolyte (▽)

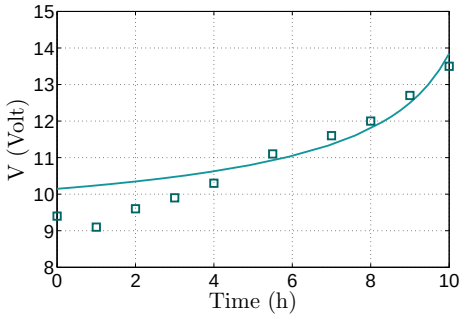

Figure 4.9: Succinic acid Voltage in the anolyte and the catholyte versus time for 0.25 M 0.57 A

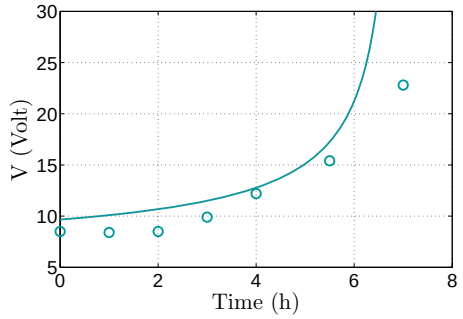

Figure 4.10: Lactic acid Voltage in the anolyte and the catholyte versus time for 0.25 M 0.57 A

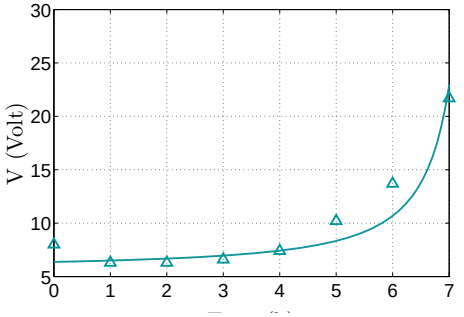

Figure 4.11: Formic acid Voltage in the anolyte and the catholyte versus time for 0.25 M 0.57 A

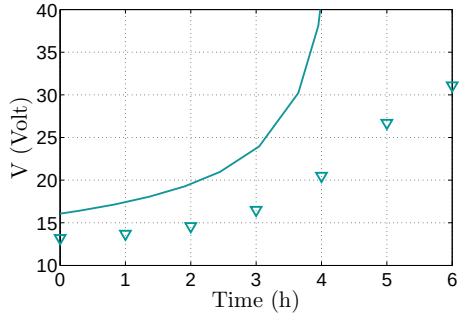

Figure 4.12: Acetic acid Voltage in the anolyte and the catholyte versus time for 0.25 M 0.57 A

Chapter 5

Conclusions & Future Work

In this thesis, we investigated the recovery of four short-chain carboxylic acids *via* electrodialysis.

It was observed that ions were able to cross this membrane easily under the applied potential gradient of 0.57 A. At 8h of the process about 81.3% recovery of succinic acid was achieved when the initial concentrations was 0.25 M. At 4-6 h of process 86.0%, 82.0%, 81.0% for acetic acid, formic acid and lactic acid was recovered, respectively.

In addition, the energy consumption and current efficiency values for the recovery of the four carboxylic acids were observed to be about 4.8 - 6.3 kWh/kg and 95.3% for succinic acid 0.25 M, 8.26 - 10.84 kWh/kg and 81% for acetic acid, 8.3- 10.8 kWh/kg and 75% for formic acid and 4.58 - 8.75 kWh/kg and 87.8% for lactic acid.

The fact that these energy consumption values are on the higher level than those reported in literature indicates the need to develop a more efficient anionexchange membrane with low resistance and high selectivity to reduce energy consumption and enhance current efficiency of the process and to study the restrictions by the concentration polarisation phenomena.

In order to create a prediction model of the concentration values based on the current, we calculated the parametres with LSM based on Kohlraush's law and the initial experimental data. We created four equations one for each carboxylic acid. Those equations describe really well the production of the four carboxylic acids as we observed when we compared them with the experimental data. Thus, those equations can be very useful in future experiments as a guide.

We investigated also the recovery of SCCAs from mixture solutions and we observed that the recovery percentage of all acids from the mixture exclude from the ones of clean aqueous solutions with the succinic acid clear aqueous solution having the smallest deviation compared to the mixture.

The acids fluxes were calculated for succinic acid, lactic acid, formic acid and acetic acid. We observed that for every acid the J values have a linear relationship to the electric quantity through the membrane cell and the flux was increased for higher concentration. Succinic acid had the maximum flux of 0.34 $g{\cdot}s^{-1}{\cdot}m^{-2}$, followed by lactic acid with a maximum flux of 0.23 $g{\cdot}s^{-1}{\cdot}m^{-2}$ and acetic and formic acid with maximum fluxes of 0.16 $g{\cdot}s^{-1}{\cdot}m^{-2}$ and 0.14 $g{\cdot}s^{-1}{\cdot}m^{-2}$, respectively. Comparing our results with the existing literature we observed that we were able to obtain high values of flux.

Additionally, we developed a dynamic model, the models presented in this thesis were able to fit the experimental data quite well despite some small deviations and they can be employed for the prediction of carboxylic acid's recovery. Predictions were made for the concentrations in the anolyte and in the catholyte, for volumes, voltage, power and energy consumption. We could predict changes in the concentrations in the anolyte and in the catholyte, and voltage values very accurately for succinic acid and formic acid and for acetic acid and lactic acid we observed some discrepancies when we compared them with the experimental data, this may well be due to the problems in operation rather than in modeling.

Although the applicability of this technique has been demonstrated for several carboxylates, there are still many things that need further research. Improving antifouling characteristics and increase selectivity for co-ions are the main application-related optimisation goals [13]. Future work can focus on performing analysis for the complete system, including the bioreactor and the study of the robustness of the model in order to extract the corresponding acids in a simple manner with higher efficiency and recovery ratio as well as lower energy consumption. Moreover, the cost of the membranes needs to be reduced in order to broaden the application [48].

Bibliography

[1] Apostolis A. Koutinas, Kookos K. Ioannis, Optimisation of processes and systems with applications in MATLAB and GAMS. Tziolas Publications, (2013).

[2] Stephen J. Andersen, Korneel Rabaey, Jiajie Xu, Juan J. L., Guzman and Largus T. Angenent. In-line and selective phase separation of medium-chain carboxylic acids using membrane electrolysis. Chem. Commun, 51 (2015) 6847-6850 .

[3] Generalic et al., http://glossary.periodni.com/glossary.electrodialysis, (2017).

[4] Nemecek et al., http://vscht.cz/kat/download/laboratoryelectrodialysis, (2017).

[5] A.C. Fisher, Department of Chemical Engineering and Biotechnology, Univ. of Cambridge, http://www.ceb.cam.ac.uk/research/groups/rg-eme/teaching-notes/mass-transport, Department of Chemical Engineering and Biotechnology, Univ. of Cambridge,(2017),

[6] Salah Benslimane, Ridha Zerdoumi, Kafia Oulmia, Electrochemical characterization of the cmx cation exchange membrane in buffered solutions: Effect on concentration polarization and counterions transport properties, Desalination, 340(1) (2014) 42-48.

[7] Genu and Green, Bio-based products over petroleum-based products, https://denmarkusmgreentour.wordpress.com/2012/07/09/bio-based-products-over-petroleum-based-products, (2012).

[8] G.R. Petersen, J.J. Bozell. Technology development for the production of biobased products from biorefinery carbohydrates -the us department of energy "top 10" revisited. Green Chem., 12 (2010) 539-554.

[9] Marcel Mulder, Basic Principles of Membrane Technology. Kluwer Academic Publishers, (1996).

[10] T. S.Davis, Handbook of Industrial Membrane Technology, Noyes Publication, (1990).

[11] H. Strathmann. Electrodialysis,a mature technology with a multitude of new applications. Desalination, 264 (2010) 268 .

[12] M. Molzahn, Rafiqul Gani, Ryzhard Pohorecki, John Bridgwater and Crispulo Gallegos, Chemical Engineering and Chemical Process Technology, EOLSS Publications, (2010).

[13] Yaping Zhang, Yanhong Xue, Guangwen Chen Chuanhui Huang, Tongwen Xu, Application of electrodialysis to the production of organic acids: State-of-the-art and recent developments. Journal of Membrane Science, 288, 1-12, (2007).

[14] W. Ostwald,Elektrische eigenschaften halbdurchlassiger scheidewande, Journal of Physik. Chem, 6 (1890) 71 .

[15] F.G. Donnan, Theory of membrane equilibria and membrane potentials in the presence of non-dialyzing electrolytes, Z. Elektrochem, 17 (1911) 572.

[16] Yoshinobu Tanaka, Ion-exchange membrane electrodialysis for saline water desalination and its application to seawater concentration, Industrial Engineering, (2011) 494-7503 .

[17] H. Strathmann, Electrodialytic membrane processes and the practical application. Studies in Environmental Sciencel,(1994) 495-533.

[18] Cornelis Ronald Visser, Electrodialytic Recovery of Acids and Bases, PhD thesis, (2001).

[19] Ugur Kurta, Yasar Avsara, Talha Gonullu, Fatih Ilhana, Harun Akif Kabuka, Recovery of mixed acid and base from wastewater with bipolar membrane, Desalination and Water Treatment,(2014) 1-9.

[20] Larry R. Faulkner, Allen J. Bard, Electrochemical Methods-Fundamentals and applications, John Wiley and Sons, (2001).

[21] J.J. Krol. Monopolar and bipolar ion exchange membranes, PhD thesis, (1997).

[22] Ekaterina Nevakshenova, Kseniya Nebavskaya Natalia Pismenskaya, Nadezhda Melnik and Victor Nikonenko. Enhancing ion transfer in overlimiting electrodialysis of dilute solutions by modifying the surface of heterogeneous ion-exchange membranes, International Journal of Chemical Engineering, (2012).

[23] Seung-Hyeon Moon Hong-Joo Leea, Heiner Strathmann, Determination of the limiting current density in electrodialysis desalination as an empirical function of linear velocity, Desalination, 190 (2006) 43-50.

[24] G. S. Gohil, Arunima Saxena, and Vinod K. Shahi, Electrochemical membrane reactor: Single-step separation and ion substitution for the recovery of lactic acid from lactate salts, Ind. Eng. Chem. Res., 46 (2007) 1270-1276.

[25] Pierre Fabry, Christine Lefrou and Jean-Claude Poignet, L electrochimie-Fondamentaux avec exercices corriges, EDP Sciences, Grenoble Sciences collection, (2009).

[26] Botho von Schwerin, Zeitschrift fur electrochemie, Journal of Bd, 23 (1917) 126-130 .

[27] G. Kraaijeveld et al., Modeling electrodialysis using maxwell-stefan description, The Chemical Engineering Journal, 57 (1995) 163-176 .

[28] G. Nano,B. Mazza, N. Boniardi, R. Rota, Lactic acid production by electrodialysis part ii modelling, Journal of applied biochemistry, 27 (1996) 135-145.

[29] Yong Keun Changa, Ik-Keun Yooa, Ho Nam Changa, Eun Gyo Leea, Seung-Hyeon Moonb, Lactic acid recovery using two-stage electrodialysis and its modelling, Journal of Membrane Sciencey, 145 (1998).

[30] Mauro Moresi, Marcello Fidaleo, Modelling the electrodialytic recovery of sodium lactate, Biotechnol. Appl. Biochem, 40 (2004).

[31] N. Aziz, F.S. Rohman, M.R. Othman, Modeling of batch electrodialysis for hydrochloric acid recovery, The Chemical Engineering Journal, 162 (2010) 466-479.

[32] Michal Pribyl, Petr Cervenka, Jifi Hrdlicka and Dalimil Snita, Mathematical modeling of electrochemical cell involving novel kinetics description, (2011).

[33] Paul K. Andersen, Azadeh Ghorbani, Abbas Ghassemi and Reza Foudazi, A prediction model of mass transfer through an electrodialysis cell, Desalination and Water Treatment, (2016).

[34] Kannan Pakshirajan, Satinder Kaur Brar, Saurabh JyotiSarma, Platform Chemical Biorefinery:Future Green Chemistry, Elsevier, (2016).

[35] Chrysanthi Pateraki, Maria Patsalou, Anestis Vlysidis, Nikolaos Kopsahelis, Colin Webb, Apostolis A. Koutinas and Michalis Koutinas, Actinobacillus succinogenes : Advances,on,succinic acid production and prospects for development of integrated biorefineries, Biochemical Engineering Journal,112 (2016) 285-303

[36] Xu Tongwen, Electrodialysis processes with bipolar membranes (edbm) in environmental protection, Resources Conservation and Recycling, 37 (2002) 1-22 .

[37] K.I. Kikuchii, H. Takahashi, K. Ohba, Sorption of mono-carboxylic acids by an anion-exchange membrane, Biochem. Eng. J,16 (2003) 311-315.

[38] J.A. Dean, Lange's Handbook of Chemistry. McGraw-Hill Book Co, (1985).

[39] G. Durand, M. Rakib, J.S.J. Ferrer, S. Laborie, Formic acid regeneration by electromembrane process. Journal of Membrane Science, 280 (2006) 509-516 .

[40] Y.Y. Lee, A.P. Zeng, H.W. Ryu, Y.J. Wee, J.S. Yun, Recovery of lactic acid by repeated batch electrodialysis and lactic acid production using electrodialysis wastewater,-Journal of Bioscience and Bioengineering, 99 (2005) 104-108.

[41] Vinod K. Shahi, R.K. Nagarale, G.S. Gohil, Recent developments on ion-exchange membranes and electro-membrane processes, Advances in Colloid and Interface Science, 119 (2006) 97-130.

[42] S.P. Tsa, P.J. Moon, S.J. Parulekar, Competitive anion transport in desalting of mixtures of organic acids by batch electrodialysis,Journal of Membrane Science, 141 (1998) 75-89.

[43] Philip Murra, Electrodialysis and Electrodialysis Reversal, American Water Works Association, (1995).

[44] Ping Yu, Zhixin Wang, Yunbai Luo, Recovery of organic acids from waste salt solutions derived from the manufacture of cyclohexanone by electrodialysis, Journal of Membrane Science, 280 (2006) 134-137.

[45] Richard W. Baker, Membrane Technology and Applications, John Wiley & Sons, Ltd., (1995).

[46] David A. Glassner et al, Recovery of carboxylic acids produced by fermentation, Applied Biochemistry and Biotechnology, 51 (1995) 73-82 .

[47] Durda Vasic, Racki Bruno Zelic. Recovery of puryvic acid from fermentation broth: process development and modeling, Desalination, 174 (2005) 267-276.

[48] Adrie J.J., Straathof Camilo, S. Lopez Garzon, Recovery of carboxylic acids produced by fermentation, Biotechnology Advances, 32 (2014) 873-904.

**

Appendix A

Experimental data

Table A.1: Measurements of Suc. Acid 0.25M

t (h)	m_c (g)	V_c (mL)	m_a (g)	V_a (mL)	Mass Bal.(g)
0	14,340	500	0,000	100	14,340
3,5	14,014	498	0,098	98,5	14,111
7	13,987	496	0,120	97	14,107
8	13,822	494	0,135	95,5	13,957
23,3	13,687	492	0,327	94	14,015
24	13,245	490	0,334	93	13,579

Table A.2: Measurements of Suc. Acid 0.25 M 0.57 A 10 h

t (h)	V(V)	C(A)	V_c (mL)	m_c (g)	V_a (mL)	m_a (g)	Mass Bal.(g)
0	9,4	0,57	500	13,78	200	0,12	13,90
1	9,1	0,57	499	12,84	216	0,94	13,79
2	9,6	0,57	498	11,28	215	2,52	13,80
3	9,9	0,57	497	9,69	214	3,85	13,53
4	10,3	0,57	494	8,30	213	5,27	13,58
5,5	11,1	0,57	479	5,69	212	7,49	13,18
7	11,6	0,57	478	3,72	211	9,44	13,16
8	12	0,57	476	2,58	216	10,80	13,38
9	12,7	0,57	474	1,59	215	11,67	13,27
10	13,5	0,57	470	0,92	220	12,14	13,05

Table A.3: Succinic acid concentration in the anolyte and the catholyte versus time for 0.5 M 0.57 A 10 h

t (h)	V(V)	C(A)	V_c (mL)	m_c (g)	V_a (mL)	m_a (g)	Mass Bal.(g)
0	9,4	0,57	500	29,05	200	0,11	29,16
1	9,1	0,5	499	27,59	216	0,88	28,47
2	9,6	0,57	498	25,86	215	2,42	28,28
3	9,9	0,57	497	24,60	214	3,71	28,30
4	10,3	0,57	494	22,85	213	5,66	28,51
5,5	11,1	0,57	479	21,35	212	7,36	28,71
7	11,6	0,57	478	18,27	211	10,37	28,64
8	12	0,57	476	16,52	216	11,86	28,38
9	12,7	0,57	474	14,59	215	13,84	28,43
10	13,5	0,57	470	13,26	220	15,05	28,32

Table A.4: Acetic acid concentration in the anolyte and the catholyte versus time for 0.25 M 0.57 A 6 h

t (h)	V(V)	C(A)	V_c (mL)	m_c (g)	V_a (mL)	m_a (g)	Mass Bal.(g)
0	13,2	0,5	500	6,4	200	0	6,400
1	13,7	0,57	491	5,11622	207	0,92322	6,039
2	14,6	0,57	489	3,94134	207	2,1114	6,053
3	16,5	0,57	484	2,6862	210	3,3348	6,021
4	20,5	0,57	482	1,63398	213	4,35372	5,988
5	26,7	0,57	476	0,84252	214	5,21946	6,062
6	31,1	0,57	470	0,4089	215	5,6932	6,102

Table A.5: Formic acid concentration in the anolyte and the catholyte versus time for 0.25 M 0.57 A 7 h

t (h)	V(V)	C(A)	V_c (mL)	m_c (g)	V_a (mL)	m_a (g)	Mass Bal.(g)
0	8	0,57	500	5,81	200	0,132	5,942
1	6,3	0,57	499	4,92014	216	0,85752	5,778
2	6,3	0,57	498	3,84954	215	1,8103	5,660
3	6,6	0,57	497	2,89751	214	2,65788	5,555
4	7,4	0,57	496	2,01376	213	3,39522	5,409
5	10,2	0,57	495	1,3563	212	3,9962	5,353
6	13,7	0,57	494	1,0127	211	4,55971	5,572
7	21,7	0,57	493	0,5423	216	5,01768	5,560

Table A.6: Lactic acid concentration in the anolyte and the catholyte versus time for 0.25 M 0.57 A 8 h

t (h)	V(V)	C(A)	V_c (mL)	m_c (g)	V_a (mL)	m_a (g)	Mass Bal.(g)
0	8,5	0,57	500	8,335	200	0	8,335
1	8,4	0,5	499	6,92612	216	1,33056	8,257
2	8,5	0,57	498	4,86048	215	3,3325	8,193
3	9,9	0,57	497	2,99691	214	5,18736	8,184
4	12,2	0,57	496	1,62192	213	6,73293	8,355
5,5	15,4	0,57	495	1,0395	212	7,12744	8,167
7	22,8	0,57	494	0,7904	211	7,57068	8,361
8	30,1	0,57	493	0,27608	216	8,09568	8,372

Table A.7: Acid solution mixture concentration in the anolyte and the catholyte versus time for 0.25 M 1.12 A 8 h

t (h)	V (V)	C (A)	V_c (mL)	V_a (mL)	m_c suc. (g)	m_a suc. (g)	m_c lac. (g)	m_a lac. (g)	m_c for. (g)	m_a for. (g)	m_c ace. (g)	m_a ace. (g)	MB suc. (g)	MB ace. (g)	MB for. (g)	MB ace. (g)
0	13,2	1,11	500	200	14,71	0,61	4,50	0,12	5,85	0,284	5,98	0,10	15,32	4,61	6,134	6,08
1,2	10,3	1,11	499	199	13,56	1,74	3,88	0,49	5,18	1,05	5,54	0,51	15,30	4,38	6,24	6,04
2,1	10,2	1,11	498	198	12,45	2,66	3,67	0,77	4,54	1,62	5,23	0,81	15,11	4,44	6,17	6,04
3,4	10,9	1,11	497	202	10,85	4,10	3,29	1,27	3,57	2,51	4,72	1,23	14,96	4,55	6,09	5,95
4,3	11,4	1,11	485	214	9,47	5,09	2,93	1,56	2,98	3,04	4,23	1,59	14,56	4,50	6,03	5,82
5,1	12,2	1,11	475	224	7,83	6,19	2,55	1,91	2,48	3,69	3,71	1,93	14,03	4,46	6,18	5,63
6,3	13,2	1,11	474	225	6,06	8,01	2,14	2,36	1,61	4,25	2,99	2,59	14,07	4,51	5,86	5,58
7	13,9	1,11	472	227	5,09	9,23	1,88	2,61	1,32	4,56	2,50	3,02	14,33	4,50	5,88	5,52
8	15,4	1,11	435	264	3,37	11,1	1,46	3,09	0,95	5,33	1,87	3,75	14,46	4,55	6,29	5,61

Table A.8: Acid solution mixture concentration in the anolyte and the catholyte versus time for 0.5 M 1.12 A 12 h

t (h)	V (V)	C (A)	V_c (mL)	V_a (mL)	m_c suc. (g)	m_a suc. (g)	m_c lac. (g)	m_a lac. (g)	m_c for. (g)	m_a for. (g)	m_c ace. (g)	m_a ace. (g)	MB suc. (g)	MB ace. (g)	MB for. (g)	MB ace. (g)
0	13,6	1,12	500	200	28,44	0,14	11,27	0,67	10,51	0	14,95	0	28,58	11,94	10,51	14,95
1	9,3	1,12	499	199	27,38	0,84	10,69	1,28	9,66	0,79	14,22	0,20	28,21	11,97	10,44	14,42
2	9,2	1,12	498	198	26,49	1,81	10,18	1,90	8,32	1,88	13,47	0,44	28,30	12,08	10,20	13,91
3	9,1	1,12	496	204	25,30	3,03	9,40	2,20	7,41	2,99	13,39	0,81	28,33	11,60	10,40	14,20
4	9,2	1,12	495	205	24,51	4,01	8,69	2,36	6,56	3,74	13,31	0,86	28,52	11,05	10,30	14,17
5	9,1	1,12	494	206	23,14	5,16	8,20	2,73	5,80	4,58	13,14	1,11	28,31	10,93	10,38	14,25
5,58	9,8	1,12	493	207	22,77	6,28	7,74	3,21	5,04	5,39	12,82	1,72	29,04	10,95	10,43	14,54
8	10,2	1,12	492	208	19,31	8,43	6,84	4,00	3,09	7,05	12,63	2,13	27,74	10,84	10,14	14,76
8,83	10,2	1,12	491	209	18,44	9,73	6,48	4,28	2,77	8,17	12,13	2,21	28,17	10,77	10,94	14,34
11,17	11,1	1,12	490	210	14,16	12,94	5,49	5,38	1,73	8,43	11,71	2,77	27,10	10,86	10,16	14,48
12,17	11,4	1,12	450	250	11,10	15,97	4,40	6,48	0,58	9,89	9,31	3,64	27,07	10,88	10,47	14,94

Appendix B

Current-Voltage Curves and pH measurements

The following power supply was used to establishe the current: power supply (HY6003D, Automation Technology Inc., Hoffman Estates, IL).

Current-voltage curves were determined by a stepwise increase of the current density through the cell (steps of ≈ 0.3 A). After a current increase the system was allowed to reach steady state after which the voltage was measured, followed by the next current increase. We performed measurements of four different concentrations of NaCl (0.05 M, 0.1 M, 0.2 M, 1M) in the catholyte and Na_2HPO_4 1 M in the anolyte and measurements with tap water. The volume of the solutions flowing through the two central compartments was 500 mL. The flowrate of each stream was adjusted to 3 L/h.

The pH measurements were performed by applying a constant current density as a function of time and we performed measurements for three different concentrations of NaCl (0.05 M, 0.1 M, 0.2 M). We know that the Ph of the solutions remains constant when a current density smaller or equal to the limiting current density is applied.

Ion transport through monopolar ion exchange membranes

1 Current - voltage curves

Below, we present the measurements with NaCl and tap water that were conducted in the electrochemical cell.

The measurements of three different concentrations of NaCl (0.05 M, 0.1 M, 0.2 M)in the catholyte and Na_2HPO_4 1 M in the anolyte are presented in Fig. B.1, the measurements with tap water in Fig. B.2 and those with NaCl 1 M in Fig. B.3. We can observe that in Fig. B.1 and B.2 the three regions which have been previously described can not be detected. Comparing those diagrams with other experimental data that can be found in the literature, we can observe higher voltage measurements and this is due either to the membrane's resistance or to the connectivity of the electrochemical cell. Furthermore we observe that three regions appear for smaller values of voltage that we can't measure with

our power supply. Finally, the resistance's values of the electrochemical cell are presented in Fig. B.4 for each experiment which are also high in comparison with respective ones that can be found in the literature.

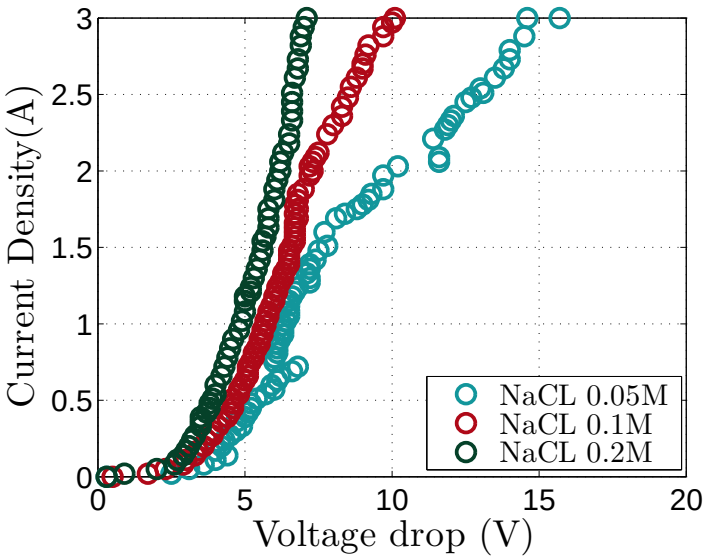

Figure B.1: Current-voltage curve measured in a 1 M NaCl solution showing the occurrence of a limiting current density (Ilim) and the presence of the three distinct regions.

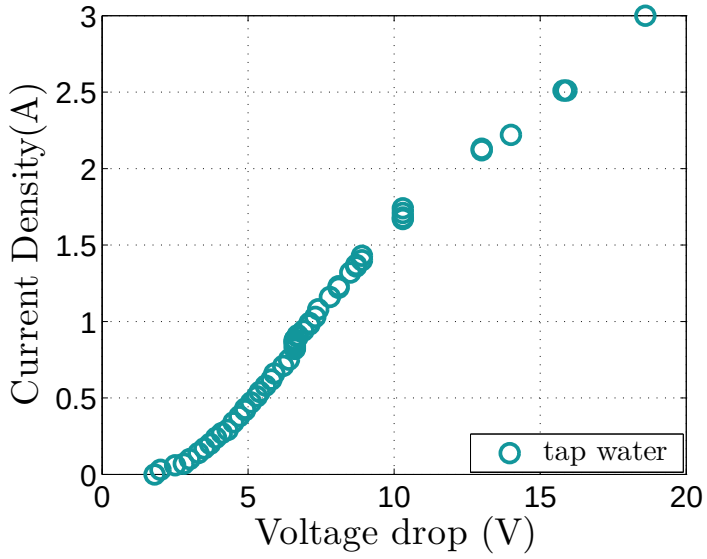

Figure B.2: Influence of bulk NaCl concentration on the current-voltage curve

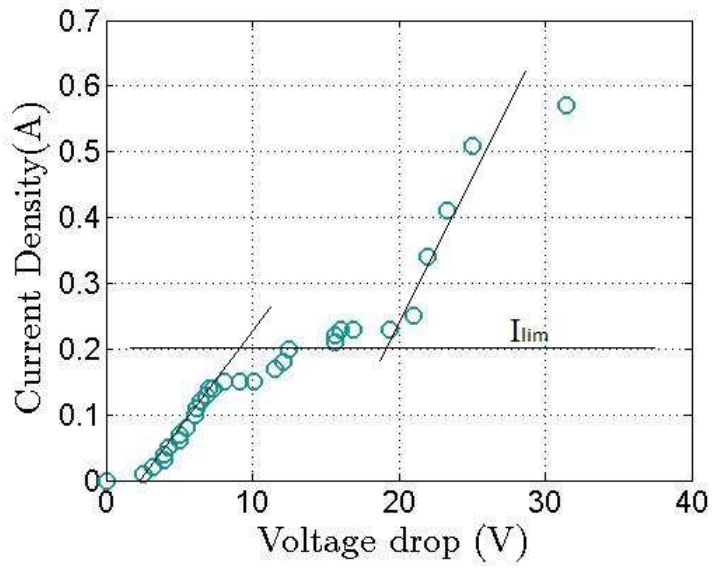

Figure B.3: Current-voltage curve of tap water

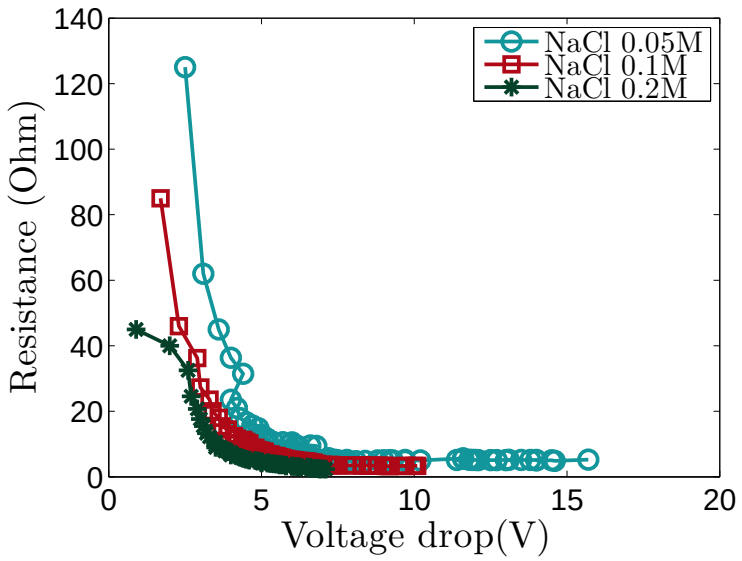

Figure B.4: Resistance-voltage curve measured in a 0.05 M, 0.1 M, 0.2 M NaCl solution.

2 pH measurements

The measurements of three different concentrations of NaCl (0.05 M, 0.1 M, 0.2 M) are presented in Fig. B.5 - Fig. B.7.

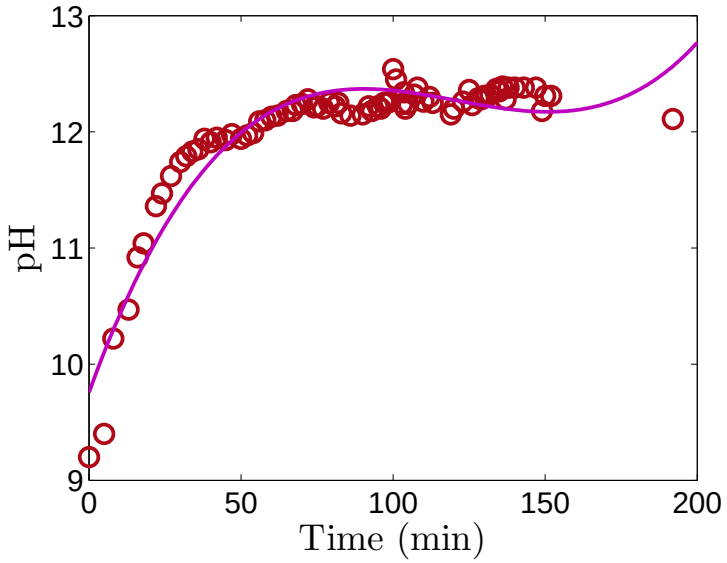

Figure B.5: Change in solution pH as a function of time, NaCl 0.05M

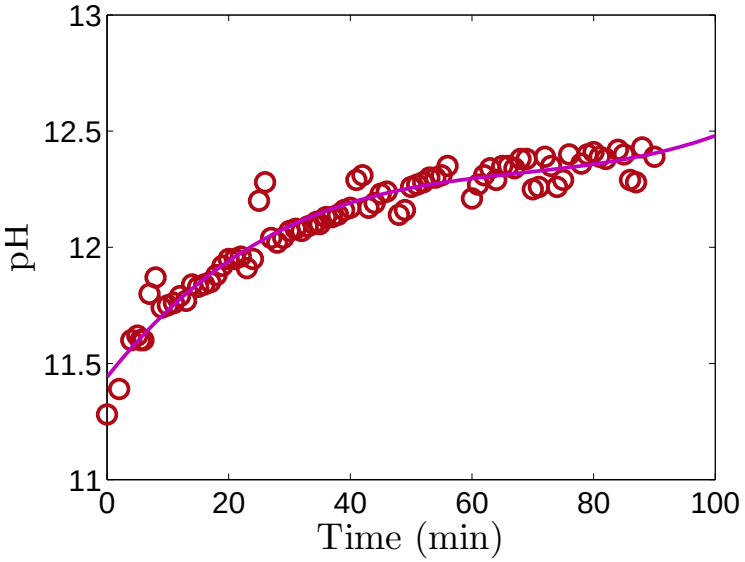

Figure B.6: Change in solution pH as a function of time, NaCl 0.1M

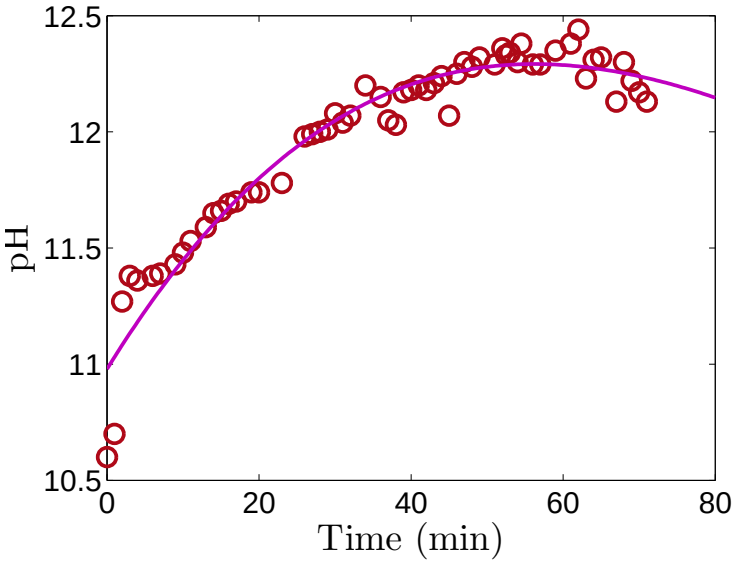

Figure B.7: Change in solution pH as a function of time, NaCl 0.2M

3 Experiments with NaCl 1 M in the anolyte

The measurements of three different concentrations of NaCl (0.05 M, 0.1 M, 0.2 M) in the catholyte and NaCl 1 M in the anolyte are presented in Fig. B.8. The resistance's values of the electrochemical cell are presented in Fig. B.9.

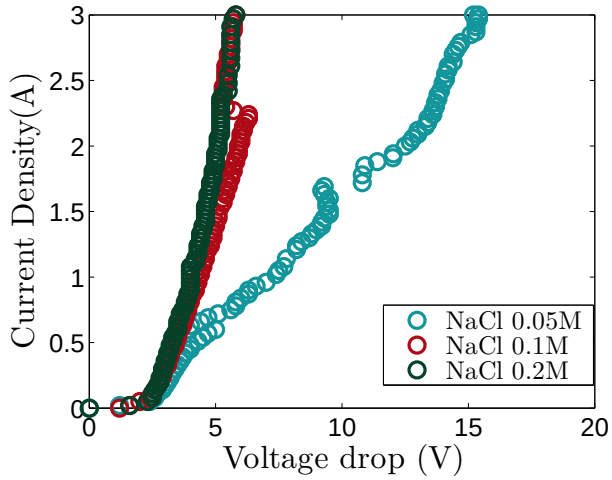

Figure B.8: Influence of bulk NaCl concentration on the current-voltage curve with NaCl 1 M in the anolyte

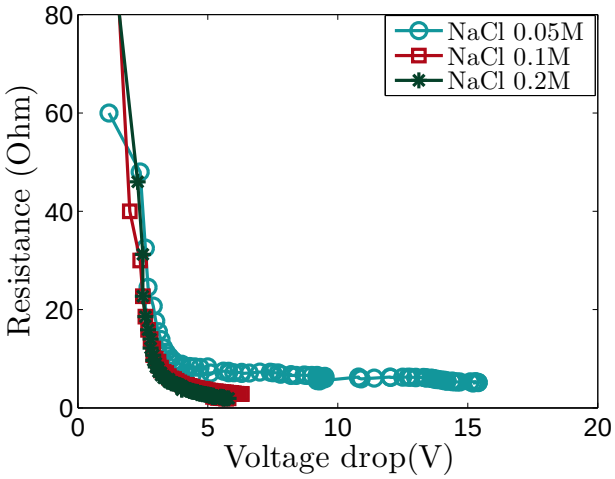

Figure B.9: Resistance-voltage curve measured in a 0.05 M, 0.1 M, 0.2 M NaCl solution with NaCl 1 M in the anolyte

4 pH measurements with NaCl 1 M in the anolyte

The measurements of three different concentrations of NaCl (0.05 M, 0.1 M, 0.2 M) in the catholyte and NaCl 1 M in the anolyte, are presented in Fig. B.10 and in Fig. B.11.

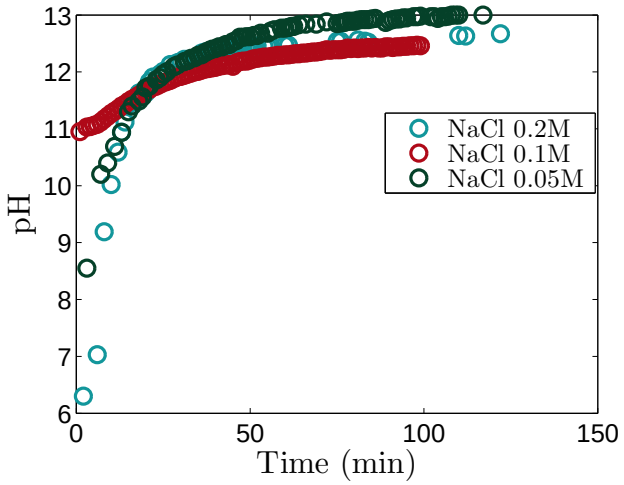

Figure B.10: Change in solution pH of the catholyte as a function of time

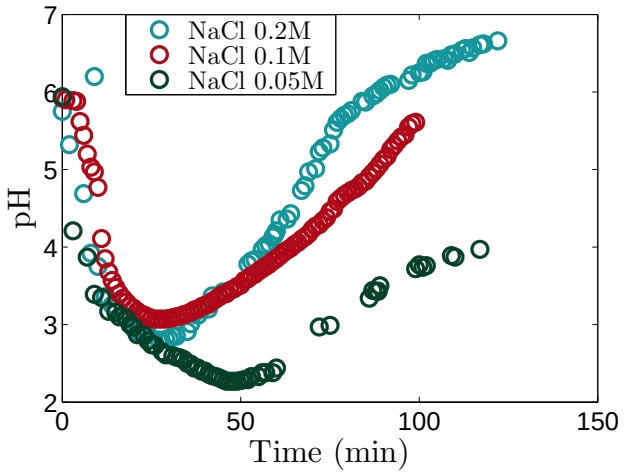

Figure B.11: Change in solution pH of the anolyte as a function of time

Appendix C

Experiments to calculate pumps flow rate

In order to characterize our experimental set up, we performed four set of measurements to calculate the pump's flow rate. The measurements are presented in Tb. C.1 and the results are presented in Tb. C.2 .

As we can see the flow rate for Pump A was 3.64 L/h and for Pump B was 3.03 L/h.

Table C.1: Measurements to calculate the pump's flow rate

	PumpB	**PumpA**	**PumpB**	**PumpA**	**PumpB**	**PumpA**
mL	Sum (sec)	Sum (sec)	Sum (h)	Sum (h)	flow rate (mL/h)	flow rate (mL/h)
100	106,5	104,5	0,030	0,029	3380,282	3444,976
200	230	240	0,064	0,067	3130,435	3000,000
300	245,25	409,5	0,068	0,114	4403,670	2637,363

Table C.2: Flow rate

	Pump A:	**Pump B:**
flow rate(mL/h)	3638,13	3027,45
flow rate(L/h)	3,64	3,03

Appendix D

Matlab codes

Matlab code-LSM

Mathworks Matlab code used for the linear least squares estimation of the parameters of the model.

```
\begin{flushleft}
% function [theta,vci,R_sq,t_val,t_crit,pvals]=LSM(X,y,alfa)


%susuc 0.25 0.57
X=[1 4.28; 1 4.59; 1 5.21; 1 6.06; 1 7.02; 1
9.95; 1 15.18; 1 21.83; 1 35.15; 1  60.56];%1 1/sqr(C)
y=[16.49 15.96 16.84 17.37 18.07 19.47 20.35 21.05 22.28 23.68 ]'; %R


%suc0.5
%X=[1 2.14; 1 2.27; 1 2.39; 1 2.56; 1 2.74; 1 3.19; 1 3.52; 1  3.98; 1 4.37];
%y=[ 17.89 19.65 20.53 20.70 21.05 21.75 21.93 22.63 22.81 ]';



%acetic0.25

% X=[1 3.60; 1 4.42; 1 5.71 ; 1 8.29; 1 13.58; 126.01; 1 52.91];
% y=[ 23.16 24.04 25.61 28.95 35.96 46.84 54.56 ]';


%formic025
% %
% X=[ 1 3.96; 1 4.67; 1  5.95; 1 7.90; 1 11.34;
  1  16.80;1 22.45; 1 41.85];
% y=[ 14.04 11.05 11.05 11.58 12.98 17.89 24.04 38.07]';
```

```
% lactic025

%X=[ 1 2.76; 1 3.32; 1 4.72; 1 7.63; 1 14.08;
1 21.92; 1 28.77; 1 82.20];
%y=[ 14.91 14.74 14.91 17.37 21.40 27.02 40.00 52.81]';


%for i=0.7:0.01:0.8

X(:,2)=X(:,2).^0.7;
%ni=i

%n number of experimental points k parametres to estimate -1
[n,k]=size(X);
k=k-1;
alfa=0.5;

theta_LS=inv(X'*X)*X'*y

P=X*inv(X'*X)*X';
e=(eye(n)-P)*y;
Jn=ones(n);

SSE=y'*y-theta_LS'*X'*y;
SST=y'*y-y'*Jn*y/n;
SSR= theta_LS'*X'*y-y'*Jn*y/n;


R_sq=SSR/SST %R^2

s_sq=SSE/(n-(k+1)); %s^2

%the estimation of parametres
s=sqrt(s_sq);
C=inv(X'*X);
se=s*sqrt(diag(C));

% 95%
t_crta empostosinis=tinv(1-(alfa/2),n-(k+1));
theta_vci=t_crt*se;
t_val=theta_LS./se;

%p values
```

```
pvals = 2 * tcdf(-abs(t_val), n-(k+1));



for i=1:250
z(i)=i;

ypred(i)=theta_LS(2)*(z(i))+theta_LS(1);

end

%
% %end
```

Matlab code-Dynamic Model

This is an example of the MAtlab code we used for succinic acid.

```
clear all

%EXPERIMENTAL DATA


DATA=[  0       8       0.57    500     5.81    200     0.132   5.942   0
1       6.3     0.57    499     4.92014 216     0.85752 5.778   2.77
2       6.3     0.57    498     3.84954 215     1.8103  5.660   4.75
3       6.6     0.57    497     2.89751 214     2.65788 5.555   6.51
4       7.4     0.57    496     2.01376 213     3.39522 5.409   8.97
5       10.2    0.57    495     1.3563  212     3.9962  5.353   9.92
6       13.7    0.57    494     1.0127  211     4.55971 5.572   6.22
7       21.7    0.57    493     0.5423  216     5.01768 5.560   6.43

];
par=[0.772
     10.1265
          4.3523]

% lb=[0.5; 0.5; 0.5]
% ub=[1.0; 1.5; 5]
% %PAR=fmincon(@ObjFun,par,[],[],[],[],lb,ub,[],options,DATA)
% [fopt,PAR,istate]=sa('ObjFun',par,lb,ub,10,10,1000,0.85,10,4,1e-6,DATA)
%
%
 ......................
```

```
% THE REST IS JUST TO PLOT EXPERIMENTA
 DATA AND THEORETICAL PREDICTIONS
% FOR COMPARISON ..............................................

hta   =  par(1)   % electrical efficiency
alfa  = par(2)
beta  =  par(3)

omega = 1   ;   % electroosmosis coef
  in mol W / mol SA
n     =  1.4;
%
texp =DATA(:,1);
Vexp =DATA(:,2);
Iexp =DATA(:,3);
V1exp=DATA(:,4);
m1exp=DATA(:,5);
V2exp=DATA(:,6);
m2exp=DATA(:,7);

rho_w = 55.50; % molar density of water in mol/L
MW_w  = 18.015;% molar weight of water
rho_SA= 26.50; % molar density of SA    in mol/L
MW_SA = 118.09;% molar weight of SA
z_SA  = 2;
F     = 96485;
%
I     = Iexp(1); % A
C1=(m1exp(1)/MW_SA) / (V1exp(1)/1000); % mol/L
V1=V1exp(1)/1000 ; % L
C2=(m2exp(1)/MW_SA) / (V2exp(1)/1000);    % mol/L
V2=V2exp(1)/1000;  % L
% initial conditions
x0(1) = V1*C1;
x0(2) = V1;
x0(3) = V2*C2;
x0(4) = V2;
x0(5) = V1*C1*MW_SA;
x0(6) = V2*C2*MW_SA;
x0(7) = hta*I/(z_SA*F);
x0(8) = alfa+beta/C1^n;
x0(9) = I*(alfa+beta/C1^n);
x0(10)= I*I*(alfa+beta/C1^n);
x0(11)= 0;
% call dae solver
```

```
MASS=zeros(length(x0),length(x0));
MASS(1,1)=1; MASS(2,2)=1; MASS(3,3)=1;MASS(4,4)=1;MASS(11,11)=1;
options=odeset('reltol',1e-4,'abstol',1e-4,'mass',MASS);
[T,Y]=ode15s(@EDmem,3600*[0 texp(length(texp))],x0,options,par,I);

figure(1)
plot(T/3600,Y(:,9),'-','Color',colour_teal)
hold on
plot(texp,Vexp,'linestyle','none','Color',my_colour,'Marker','o')
xlabel('Time (h)')
ylabel('V (Volt)')
axis([texp(1) texp(length(texp)) 5 30])
%name of the legends
grid on

figure(2)
plot(T/3600,Y(:,5),'-','Color',my_colour)
hold on
plot(texp,m1exp,'linestyle','none','Color',my_colour,'Marker','o')
xlabel('Time (h)')
ylabel('formic acid (g)')
plot(T/3600,Y(:,6),'-','Color',colour_teal)
plot(texp,m2exp,'linestyle','none','Color',colour_teal,'Marker','o')
%name of the legends
grid on
axis([texp(1) texp(length(texp)) 0 6])
ll = legend([plot(T/3600,Y(:,5),'-','
Color',my_colour) plot(T/3600,Y(:,6),'-',
'Color',colour_teal)],'\it Catholyte','\it Anolyte') ;
set(ll,'Interpreter','latex','FontSize',(16)) ;

figure(3)
plot(T/3600,Y(:,2),'-','Color',my_colour)
hold on
plot(texp,V1exp/1000,'linestyle','none','Color',my_colour,'Marker','o')
hold on
plot(T/3600,Y(:,4),'-','Color',my_colour1)
hold on
plot(texp,V2exp/1000,'linestyle','none','Color',my_colour1,'Marker','o')
xlabel('Time (h)')
ylabel('Volume (L)')
%name of the legends
grid on
axis([texp(1) texp(length(texp)) 0 .6])
ll = legend([plot(T/3600,Y(:,2),'-',
```

```
'Color',my_colour) plot(T/3600,Y(:,4),'-','Color',my_colour1)],
'\it Catholyte','\it Anolyte') ;
        set(ll,'Interpreter','latex','FontSize',(16)) ;
%
figure(4)
plot(T/3600,Y(:,10),'-','Color',my_colour1)
xlabel('Time (h)')
ylabel('P (kW)')
%name of the legends
grid on

figure(5)
plot(T/3600,Y(:,11)./(Y(:,6)-Y(1,6)),'-','Color',colour_teal)
xlabel('Time (h)')
ylabel('Spec. energy consumption (kWh/kg SA)')
%name of the legends
grid on
\end{flushleft}
```